Dr. S. Nozawa (Keio University, Tokyo, Japan) and maintained in RPMI 1640 plus 10% FBS and 1% penicillin/streptomycin. RMG-1 is invasive to the peritoneal lining tissue accompanying ascites accumulation. HUVECs were prepared as described previously (27) and maintained in EGM-2 Bulletkit EBM medium (BioWhittaker) according to the manufacturer's instructions.

Plasmids. The AAV vector plasmids used in this study were derived from the parent vector plasmid pW1 (28), harboring a lacZ expression cassette flanked by two 145-bp inverted terminal repeats of AAV. The psFlt-1 and pNeo vector plasmids were constructed by excising the *lacZ* reporter gene from the parent vector plasmid and replacing it with the 2.4-kb mouse sFlt-1 cDNA (29) and 0.8-kb neomycin-resistance gene, respectively. pIM45 is a helper plasmid containing the AAV rep and cap genes, which are required for replication and capsid formation of AAV vectors, and has no overlapping AAV sequence compared with the vector plasmid. pladeno-1, a plasmid containing the E2A, E4, and VA genes of the adenovirus genome, was used in place of helper adenovirus for AAV vector production. *Escherichia coli* DH5-α was used for plasmid DNA amplification.

***In Vitro* Transduction.** AAV vectors were produced by cotransfection of 293 cells by the calcium phosphate coprecipitation method with the vector plasmid (psFlt-1 or pNeo), the helper plasmid (pIM45), and the pladeno-1 plasmid (30). The vector titer was determined by quantitative DNA dot-blot hybridization. RMG-1 cells were transduced with 1×10^5 particles/cell of AAV-sFlt-1 and AAV-Neo, or AAV-Neo alone, and propagated in complete medium containing 100 μg/ml G418 antibiotic to select stable clones. Analyzing cell lysates for sFlt-1 expression isolated sFlt-1-expressing clones by Western blot analysis.

Western Blot Analysis. Conditioned media were generated by culturing 3×10^6 Neo-expressing cells or sFlt-1-expressing cells in 7 ml of serum-free RPMI 1640 for 72 h. Cells were lysed in a lysis buffer [10 mM Tris-HCl, 150 mM NaCl, and 1% NP40 (pH 7.6)] supplemented with 1 mM phenylmethylsulfonyl fluoride and 500 units/ml of aprotinin. Cell lysate (10 μg) or 10 μl of conditioned medium was electrophoretically separated on a 7.5% SDS-PAGE gel, transferred to a polyvinylidene difluoride membrane (Millipore), probed by rabbit polyclonal antibody to the NH_2-terminal sequence of sFlt-1, and then reacted with horseradish peroxidase-labeled antirabbit mouse antibody. Bindings were visualized with the enhanced chemiluminescence system (Amersham).

VEGF Quantitation. Conditioned medium were generated by culturing 3×10^6 RMG-1 cells in 7 ml of RPMI 1640 plus 1% FBS for 96 h. Measurement of VEGF was performed using an ELISA kit for human VEGF (Amersham) according to the manufacturer's instructions.

***In Vitro* Proliferation of the sFlt-1-expressing Cells.** Neo-expressing cells (1×10^5) or sFlt-1-expressing cells were plated in three sets of triplicate wells. The cells were enumerated at 48, 72, and 96 h after plating.

Endothelial Cell Proliferation Assay. Conditioned medium were generated by culturing 3×10^6 Neo-expressing cells or sFlt-1-expressing cells in 7 ml of serum-free RPMI 1640 for 72 h. HUVECs (2×10^4/well) were plated in triplicate wells in EBM-2 medium (BioWhittaker) plus 5% FBS containing 25% of either conditioned medium with or without 20 ng/ml VEGF (Pepro Tech). The cells were counted 5 days after plating.

Dorsal Air Sac Assay. The dorsal air sac assay was done according to a method described previously (31). A Millipore chamber (filter pore size 0.22 μm; Millipore Co.) was filled with 0.15 ml (1×10^6 cells) of cell suspension of Neo-expressing or sFlt-1-expressing cells and implanted s.c. in the dorsum of 4-week-old female BALB/c nude mice (CLEA, Tokyo, Japan). On day 5, the implanted chambers were removed from the animals. Angiogenic response was assessed under a dissecting microscope by determining the number of newly formed blood vessels longer than 3 mm with the characteristic zigzagging pattern of tumor cell-induced new vasculature in the s.c. side of the skin area that had been in contact with the chamber.

RMG-1 i.p. Xenografts. Four-week-old female BALB/c nude mice (CLEA) were inoculated i.p. with Neo-expressing or sFlt-1-expressing cells (2×10^7 cells/mouse). Mice were sacrificed 5 weeks after the inoculation. After a mouse was sacrificed, 2 ml of PBS was injected i.p., and the peritoneal fluid was totally recovered. The volume of ascites fluid was calculated by subtracting the 2 ml of PBS injected from the total fluid volume recovered. The number of tumor cells, the number of RBCs in the ascites fluid, and the number and diameter of peritoneal disseminations were determined. Tumors 2 mm in diameter were fixed in sucrose buffered 4% paraformaldehyde, and processed for 10 μm cryostat sections and air dried. The sections were stained for alkaline phosphatase, revealing the enzyme within the capillary endothelium (32). Staining was carried out for 30 min at room temperature, using an incubation medium of the following composition: 2 mg naphtol AS-BI phosphate, 0.2 ml *N,N'*-dimethyl-formamide, 9.8 ml 0.1 M Tris-HCl buffer, 10 mg Fast red violet LB. Slides were dehydrated in tetrachloroethylene and mounted. Another set of 4-week-old female BALB/c nude mice were inoculated i.p. (2×10^7 cells/mouse) with Neo-expressing or sFlt-1-expressing cells. Mice were monitored daily.

Statistics. Comparisons of the results of the endothelial cell proliferation assay and dorsal air sac assay were performed using Student's *t* test. Comparisons of the results of the *in vivo* assays were performed using the Wilcoxon signed-rank test. The statistical significance of differences in survival times among groups was determined using a Kaplan-Meier survival analysis Wilcoxon test. A value of $P < 0.05$ was considered significant.

RESULTS

Expression of sFlt-1 in RMG-1 Cells Transduced with AAV-sFlt-1. We first examined whether RMG-1 cells produce VEGF by performing an enzyme immunoassay using the conditioned medium of RMG-1 cells. The mean VEGF level in the conditioned medium was 458 pg/ml. To determine the expression of sFlt-1 protein in RMG-1 cells transduced with AAV-Neo alone or cotransduced with AAV-sFlt-1 and AAV-Neo, stable clones were isolated and characterized for protein expression. As shown by the Western blotting (Fig. 1), the clone transduced with AAV-Neo alone (Neo clone) did not express sFlt-1 protein, whereas the clone cotransduced with AAV-sFlt-1 and AAV-Neo (sFlt-1 clone) expressed sFlt-1 protein in both the cell lysate and conditioned medium.

Growth Characteristics of sFlt-1-expressing RMG-1 Cells *in Vitro*. These clones were microscopically indistinguishable and had similar growth rates *in vitro* (Fig. 2). These results demonstrate that sFlt-1 did not affect tumor cell mitogenesis *in vitro*.

Inhibitory Effects of sFlt-1 on *in Vitro* Endothelial Cell Growth. The effect of the sFlt-1 expression of sFlt-1 clone cells on the action of VEGF was estimated using *in vitro* cultures of endothelial cells. Stimulation of HUVECs with EBM culture medium including 20 ng/ml recombinant VEGF plus 25% conditioned medium from Neo clone cells for 5 days produced a 70% increase in the cell number ($P < 0.05$). This mitogenic effect of VEGF on endothelial cells was completely abrogated by the addition of conditioned medium from sFlt-1 clone cells instead of that from Neo clone cells ($P < 0.05$; Fig. 3*A*).

Inhibitory Effects of sFlt-1 on *in Vivo* Angiogenesis. The effect of sFlt-1 expression on tumor angiogenesis was examined using mouse dorsal air sac assay. Millipore chambers filled with Neo-expressing ($n = 5$) or sFlt-1-expressing ($n = 5$) cells were implanted to nude mice. As shown in Fig. 3*B*, the average number of newly formed vessels in mice implanted Millipore chambers containing sFlt-1-expressing cells (2.6/mouse) was significantly lower than in

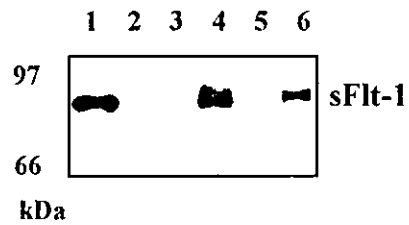

Fig. 1. Expression of sFLT-1 protein in RMG-1 cells transduced with AAV-sFlt-1. A Western blot of total cell lysates and their conditioned medium was probed with an antiserum against sFLT-1. sFLT-1 was detectable in cell lysate (*Lane 4*) and conditioned medium (*Lane 6*) of a clone transduced with AAV-sFlt-1 but not in cell lysate (*Lane 3*) and conditioned medium (*Lane 5*) of a clone transduced with AAV-Neo.

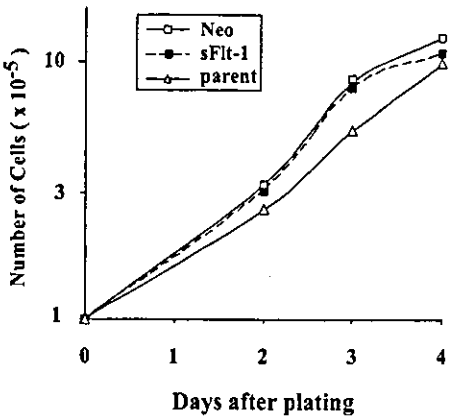

Fig. 2. *In vitro* proliferation of sFlt-1-expressing cells. The cells (1×10^5) were cultured in three sets of triplicate wells in six-well plates. The cells were enumerated at 48, 72, and 96 h after plating. The Neo-expressing cells (□) and sFlt-1-expressing cells (■) showed similar growth properties to the parent cells (△) in culture.

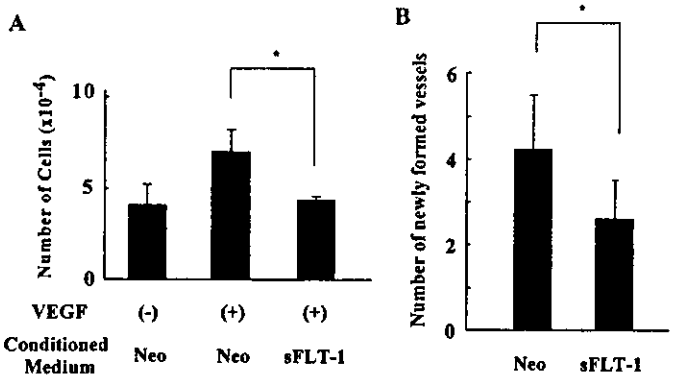

Fig. 3. *A*, suppression of VEGF-driven HUVEC proliferation by conditioned medium of sFlt-1-expressing cells. Cells were plated at 2×10^4 cells/well in 24-well plates, and 25% sFLT-1-conditioned medium or Neo-conditioned medium was added with or without 20 ng/ml recombinant human VEGF. The cells were counted after 5 days of culture. Data represent the mean of triplicate determinations; *bars*, ±SE. *B*, suppression of VEGF-driven angiogenesis *in vivo* by expression of sFlt-1. Millipore chambers filled with 0.15 ml (1×10^6 cells) of cell suspension of Neo-expressing ($n = 5$) or sFlt-1-expressing ($n = 5$) cells were implanted to nude mice. On day 5, the number of newly formed blood vessels >3 mm were counted. The average number of newly formed vessels in mice implanted Millipore chambers containing sFlt-1-expressing cells was significantly lower than in mice implanted Millipore chambers containing Neo-expressing cells. Data represent the mean; *bars*, ±SE. The statistical difference between groups was computed using Student's *t* test (*, $P < 0.05$).

mice implanted Millipore chambers containing Neo-expressing cells (4.2/mouse; $P < 0.05$). This result demonstrates that persistent expression of sFlt-1 suppressed VEGF-induced angiogenesis *in vivo*.

Suppression of Ascites Accumulation *in Vivo* and Capillary Density of the Tumors. To determine the effect of persistent sFlt-1 expression on ascites accumulation and tumorigenicity *in vivo*, either Neo-expressing ($n = 5$) or sFlt-1-expressing ($n = 5$) cells (2×10^7) were injected i.p. into nude mice. As shown in Table 1, the average volume of ascites fluid, number of tumor cells, and number of leaked RBCs in mice i.p. injected with sFlt-1 clone cells (0.07 ml; 3.83×10^5 tumor cells and 7.70×10^5 RBCs/mouse) were significantly lower than those in mice injected with Neo clone cells (1.80 ml; 3.50×10^7 tumor cells and 8.28×10^8 RBCs/mouse; $P < 0.05$). There was no significant difference in the number of peritoneal disseminations (85.6 ± 54.6 *versus* 121.4 ± 54.1). Histochemical staining of tumor sections for alkaline phosphatase showed that capillary density of the tumors. There was not a significant difference in vascularity between these groups (data not shown). The number of peritoneal disseminations >2 mm in diameter was significantly smaller in mice i.p. injected with sFlt-1 clone cells than with Neo clone cells (χ^2-statistics, $P < 0.05$). These results demonstrate that persistent expression of sFlt-1 resulted in suppression of ascites accumulation, RBC leakage, and tumor growth.

Survival Kinetics of Nude Mice Injected i.p. with sFlt-1-expressing Tumor Cells. A total of 2×10^7 Neo-expressing cells ($n = 6$) or sFlt-1-expressing cells ($n = 6$) were injected i.p. into nude mice to evaluate the effect of sFlt-1 on the mortality rate. i.p. inoculation of the parent RMG-1 cells into nude mice leads to death with reproducible kinetics (data not shown). As depicted in Fig. 4, mice injected with sFlt-1 clone cells had a median survival time of 70 days. This was significantly longer than the median survival time of 55 days of mice injected with Neo clone cells ($P < 0.05$).

DISCUSSION

In the present study, we have established an animal model of human ovarian cancer in which cancer cells persistently express sFlt-1, a selective inhibitor of VEGF. Using this model, we clearly demonstrated that nude mice inoculated i.p. with the sFlt-1-expressing cancer cells display longer survival times associated with reduced volumes of ascites.

Table 1 *The effects of sFLT-1 expression in RMG cells on ascites accumulation and peritoneal dissemination*

Four-week-old BALB/c*nu/nu* female mice were inoculated i.p. with 2×10^7 cells/mouse of either Neo-expressing cells ($n = 5$) or sFlt-1-expressing cells ($n = 5$). Mice were sacrificed 5 weeks after inoculation. After a mouse was sacrificed, ascites fluid was collected.

A. Characteristics of ascites[a]

Tumor cells	Ascites volume (ml)	RBC in ascites fluid (1×10^6/mouse)	No. of tumor cells	No. of peritoneal disseminations
Neo	1.80 ± 1.74	828 ± 534	35.0 ± 20.2	121.4 ± 54.1
sFLT-1	0.07 ± 0.03[b]	0.8 ± 0.6[b]	0.4 ± 0.2[b]	85.6 ± 54.6

B. Number of peritoneal disseminations classified by size[c]

Tumor cells	Diameter of tumors >2 mm	Diameter of tumors ≤2 mm	Total no. of mice
Neo	61	546	5
sFLT-1	19[b]	409	5

[a] The ascites volume and the number of tumor cells, RBCs in the ascites fluid, and peritoneal disseminations were measured. Data shown represent means ± SD. The statistical difference between groups was computed using Wilcoxon signed-rank test. sFLT-1 expression reduced the ascites volume, leakage of RBCs, and the number of tumor cells in the peritoneal fluid but not the number of peritoneal disseminations.

[b] $P < 0.05$.

[c] The peritoneal disseminations were counted by size. The number of peritoneal disseminations >2 mm in diameter was significantly smaller in mice i.p. injected with sFlt-1 clone cells than in mice injected with Neo clone cells ($P < 0.05$, χ^2 statistics).

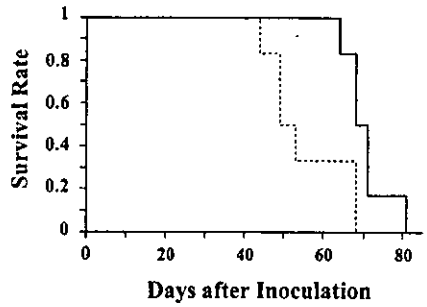

Fig. 4. Survival kinetics of nude mice injected i.p. with sFlt-1-expressing tumor cells. Four-week-old BALB/c-*nu/nu* female mice were inoculated i.p. with 2×10^7 cells/mouse of either Neo-expressing cells ($n = 6$) or sFlt-1-expressing cells ($n = 6$). Survival time was significantly greater in animals injected with tumor cells expressing sFLT-1 (solid line; $P < 0.05$, Kaplan-Meier survival analysis, Wilcoxon test) than with tumor cells expressing Neo (*dotted line*).

sFlt-1 is an endogenously expressed selective inhibitor of VEGF. It is an alternatively spliced version of the Flt-1 VEGF receptor. Inhibition of VEGF activity by sFlt-1 is mediated both by the sequestering of VEGF and by the forming of inactive heterodimers with VEGF receptors in a dominant negative fashion (23, 24). Anti-VEGF antibodies were reported to inhibit tumor growth, metastasis, and fluid accumulation of ascites tumors (33, 34). It has been additionally demonstrated that interference with VEGF-mediated angiogenesis by sFlt-1 via gene transfer inhibited tumor growth and metastasis (35–37). This approach targets the angiogenic vasculature directly, and does not require transfer of genes to each tumor cell.

It is to be noted that nude mice bearing sFlt-1-expressing cells have reduced amounts of ascites fluid despite showing no significant change in the number of peritoneal disseminations. In the light of the decreased number of RBCs in ascites fluid, we reasoned that sFlt-1 suppresses cancer-associated vascular hyperpermeability by acting on the microvasculature and thereby decreasing fluid from plasma to the peritoneal cavity (20, 33).

In this study, although VEGF-induced vascular endothelial cell mitogenesis in culture was efficiently inhibited and the number of tumor cells in the ascites fluid in mice i.p. injected with sFlt-1 clone cells was significantly low compared with the control group, there was no significant difference in the number of peritoneal disseminations. It may be that the local expression of sFlt-1 was not high enough or that the tumor cells eventually acquired the ability to increase proteolytic degradation of sFlt-1 (35). The possibility that inflammatory mediators and/or other angiogenic cytokines are involved in tumorigenicity also remains. Several human ovarian carcinomas were reported to express multiple genes that regulate angiogenesis, which was associated with the pattern of the disease and its progression (38). It is interesting to note that the number of peritoneal disseminations >2 mm in diameter was significantly smaller in mice bearing sFlt-1-expressing cancer cells than in the control, a finding consistent with the fact that tumors cannot grow to >1–2 mm^3 unless they acquire their own blood supply (4). Formation and growth of thin layers and small solid tumors of i.p. carcinomatosis may be maintained by the preexisting vasculature, whereas larger solid tumors require neovascularization for continued growth (4). Our histochemical analysis of the tumor vasculature did not reveal significant difference in vascularity of each tumor between these groups. This also reflects the fact that the decreased number of tumors, which correlated well with the result of vascular formation in dorsal air sac assay, has more biological importance, and if there is a tumor larger than a certain size, there are some levels of vascularity. The tumor vasculature in the sFlt-1-transduced group may be induced by the other tumor angiogenesis factors besides VEGF. On the other hand, we speculate that the VEGF activity was efficiently inhibited by the transgene-derived sFlt-1, because the carcinomatous ascites, which is known to be caused by VEGF-mediated angiogenesis, was almost completely suppressed. The combination of sFlt-1 gene and the other type of angiogenesis-inhibiting gene would additionally suppress the i.p. ovarian tumor formation.

Analysis of the survival kinetics of nude mice i.p. injected with tumor cells showed that persistent expression of sFlt-1 significantly prolonged survival time in tumor-bearing mice compared with the control. It is conceivable that inhibition of both ascites fluid accumulation and smaller sized disseminations may be responsible for prolongation of survival. This finding is interesting considering a previous report that pretreatment VEGF levels could be predictive of the outcome of ovarian cancers (39).

In view of the efficient inhibition of VEGF activity requiring the continuous presence of its inhibitor, sFlt-1 gene therapy could be a viable approach. AAV vectors can efficiently transduce epithelial cancer cells (40) as well as quiescent fibroblasts and muscle cells (41, 42). Given that many malignant ascites tumors are epithelial in origin, AAV vectors are suitable for this. Another advantage is that a relatively long transgene expression is expected after a single administration of recombinant AAV *in vivo* (43). In this study, transfer of the sFlt-1 cDNA to ovarian cancer cells resulted in the expression of functional sFlt-1 protein. We are currently evaluating the efficacy of *in vivo* injection of AAV-sFlt-1.

In summary, we demonstrated that stable sFlt-1 expression resulted in a reduction in the amount of ascites fluid and lengthening of survival in an ovarian cancer model, presumably by inhibiting vascular formation and permeability, and ultimately tumor growth through a mechanism of antagonizing VEGF activity.

ACKNOWLEDGMENTS

We thank Avigen, Inc. (Alameda, CA) for the AAV vector production system and Dr. S. Nozawa for RMG-1 cells.

REFERENCES

1. Ovarian cancer: screening, treatment, and follow up. NIH Consens. Statement, *12:* 1–30, 1994.
2. Parker, S. L., Tong, T., Bolden, S., and Wingo, P. A. Cancer statistics, 1996. CA Cancer J. Clin., *46:* 5–27, 1996.
3. Roszkowski, P., Wronkowski, Z., Szamborski, J., and Romejko, M. Evaluation of selected prognostic factors in ovarian cancer. Eur. J. Gynaecol. Oncol., *14:* 140–145, 1993.
4. Folkman, J. What is the evidence that tumors are angiogenesis dependent? J. Natl. Cancer Inst., *82:* 4–6, 1990.
5. Brown, H. R. Kinetics of angiogenesis in small vessels related to mouse parietal peritoneum. Anat. Rec., *184:* 364, 1976.
6. Heuser, L. S., Taylor, S. H., and Folkman, J. Prevention of carcinomatosis and bloody malignant ascites in the rat by an inhibitor of angiogenesis. J. Surg. Res., *36:* 244–250, 1984.
7. Straube, R. L. Fluid accumulation during initial stages of tumor growth. Cancer Res., *18:* 57–65, 1958.
8. Hirabayashi, K., and Graham, J. Genesis of ascites in ovarian cancer. Am. J. Obstet. Gynecol., *106:* 492–497, 1970.
9. Senger, D. R., Galli, S. J., Dvorak, A. M., Perruzzi, C. A., Harvey, V. S., and Dvorak, H. F. Tumor cells secrete a vascular permeability factor that promotes accumulation of ascites fluid. Science (Wash. DC), *219:* 983–985, 1983.
10. Garrison, R. N., Kaelin, L. D., Galloway, R. H., and Heuser, L. S. Malignant ascites. Clinical and experimental observations. Ann. Surg., *203:* 644–651, 1986.
11. Garrison, R. N., Galloway, R. H., and Heuser, L. S. Mechanisms of malignant ascites production. J. Surg. Res., *42:* 126–132, 1987.
12. Sykes, J. A. Pharmacologically active substances in malignant ascites fluid. Br. J. Pharmacol., *40:* 595P+, 1970.
13. Greenbaum, L. M., Grebow, P., Johnston, M., Prakash, A., and Semente, G. Pepstatin, an inhibitor of leukokinin formation and ascitic fluid accumulation. Cancer Res., *35:* 706–710, 1975.
14. Maeda, H., Matsumura, Y., and Kato, H. Purification and identification of [hydroxyprolyl3]bradykinin in ascitic fluid from a patient with gastric cancer. J. Biol. Chem., *263:* 16051–16054, 1988.
15. Matsumura, Y., Kimura, M., Yamamoto, T., and Maeda, H. Involvement of the kinin-generating cascade in enhanced vascular permeability in tumor tissue. Jpn. J. Cancer Res., *79:* 1327–1334, 1988.
16. Matsumura, Y., Maruo, K., Kimura, M., Yamamoto, T., Konno, T., and Maeda, H. Kinin-generating cascade in advanced cancer patients and *in vitro* study. Jpn. J. Cancer Res., *82:* 732–741, 1991.
17. White, M. J., Miller, F. N., Heuser, L. S., and Pietsch, C. G. Human malignant ascites and histamine-induced protein leakage from the normal microcirculation. Microvasc. Res., *35:* 63–72, 1988.
18. Ettinghausen, S. E., Puri, R. K., and Rosenberg, S. A. Increased vascular permeability in organs mediated by the systemic administration of lymphokine-activated killer cells and recombinant interleukin-2 in mice. J. Natl. Cancer Inst., *80:* 177–188, 1988.
19. Ohmura, E., Tsushima, T., Kamiya, Y., Okada, M., Onoda, N., Shizume, K., and Demura, H. Epidermal growth factor and transforming growth factor α induce ascitic fluid in mice. Cancer Res., *50:* 4915–4917, 1990.
20. Nagy, J. A., Morgan, E. S., Herzberg, K. T., Manseau, E. J., Dvorak, A. M., and Dvorak, H. F. Pathogenesis of ascites tumor growth: angiogenesis, vascular remodeling, and stroma formation in the peritoneal lining. Cancer Res., *55:* 376–385, 1995.
21. Shibuya, M. Role of VEGF-flt receptor system in normal and tumor angiogenesis. Adv. Cancer Res., *67:* 281–316, 1995.
22. Yamamoto, S., Konishi, I., Mandai, M., Kuroda, H., Komatsu, T., Nanbu, K., Sakahara, H., and Mori, T. Expression of vascular endothelial growth factor (VEGF) in epithelial ovarian neoplasms: correlation with clinicopathology and patient survival, and analysis of serum VEGF levels. Br. J. Cancer., *76:* 1221–1227, 1997.

23. Kendall, R. L., and Thomas, K. A. Inhibition of vascular endothelial cell growth factor activity by an endogenously encoded soluble receptor. Proc. Natl. Acad. Sci. USA, *90:* 10705–10709, 1993.
24. Kendall, R. L., Wang, G., and Thomas, K. A. Identification of a natural soluble form of the vascular endothelial growth factor receptor, FLT-1, and its heterodimerization with KDR. Biochem. Biophys. Res. Commun., *226:* 324–328, 1996.
25. Graham, F. L., Smiley, J., Russell, W. C., and Nairn, R. Characteristics of a human cell line transformed by DNA from human adenovirus type 5. J. Gen. Virol., *36:* 59–74, 1977.
26. Nozawa, S., Tsukazaki, K., Sakayori, M., Jeng, C. H., and Iizuka, R. Establishment of a human ovarian clear cell carcinoma cell line (RMG-I) and its single cell cloning–with special reference to the stem cell of the tumor. Hum. Cell., *1:* 426–435, 1988.
27. Jaffe, E. A., Nachman, R. L., Becker, C. G., and Minick, C. R. Culture of human endothelial cells derived from umbilical veins. Identification by morphologic and immunologic criteria. J. Clin. Investig., *52:* 2745–2756, 1973.
28. Fan, D. S., Ogawa, M., Fujimoto, K. I., Ikeguchi, K., Ogasawara, Y., Urabe, M., Nishizawa, M., Nakano, I., Yoshida, M., Nagatsu, I., Ichinose, H., Nagatsu, T., Kurtzman, G. J., and Ozawa, K. Behavioral recovery in 6-hydroxydopamine-lesioned rats by cotransduction of striatum with tyrosine hydroxylase and aromatic L-amino acid decarboxylase genes using two separate adeno-associated virus vectors. Hum. Gene Ther., *9:* 2527–2535, 1998.
29. Kondo, K., Hiratsuka, S., Subbalakshmi, E., Matsushime, H., and Shibuya, M. Genomic organization of the flt-1 gene encoding for vascular endothelial growth factor (VEGF) receptor-1 suggests an intimate evolutionary relationship between the 7-Ig and the 5-Ig tyrosine kinase receptors. Gene, *208:* 297–305, 1998.
30. Matsushita, T., Elliger, S., Elliger, C., Podsakoff, G., Villarreal, L., Kurtzman, G. J., Iwaki, Y., and Colosi, P. Adeno-associated virus vectors can be efficiently produced without helper virus. Gene Ther., *5:* 938–945, 1998.
31. Yonekura, K., Basaki, Y., Chikahisa, L., Okebe, S., Hashimoto, A., Miyadera, K., Wiersba, K., and Yamada, Y. UFT and its metabolites inhibit the angiogenesis induced by murine renal cell carcinoma, as determined by a dorsal air sac assay in mice. Clin. Cancer Res., *5:* 2185–91, 1999.
32. Ziada, A. M., Hudlicka, O., Tyler, K., R., and Wright, A. J. The effect of long-term vasodilatation on capillary growth and performance in rabbit heart and skeletal muscle. Cardiovasc. Res., *18:* 724–32, 1984.
33. Luo, J. C., Toyoda, M., and Shibuya, M. Differential inhibition of fluid accumulation and tumor growth in two mouse ascites tumors by an antivascular endothelial growth factor/permeability factor neutralizing antibody. Cancer Res., *58:* 2594–600, 1998.
34. Mesiano, S., Ferrara, N., and Jaffe, R. B. Role of vascular endothelial growth factor in ovarian cancer: inhibition of ascites formation by immunoneutralization. Am. J. Pathol., *153:* 1249–1256, 1998.
35. Kong, H. L., Hecht, D., Song, W., Kovesdi, I., Hackett, N. R., Yayon, A., and Crystal, R. G. Regional suppression of tumor growth by *in vivo* transfer of a cDNA encoding a secreted form of the extracellular domain of the flt-1 vascular endothelial growth factor receptor. Hum. Gene Ther., *9:* 823–833, 1998.
36. Goldman, C. K., Kendall, R. L., Cabrera, G., Soroceanu, L., Heike, Y., Gillespie, G. Y., Siegal, G. P., Mao, X., Bett, A. J., Huckle, W. R., Thomas, K. A., and Curiel, D. T. Paracrine expression of a native soluble vascular endothelial growth factor receptor inhibits tumor growth, metastasis, and mortality rate. Proc. Natl. Acad. Sci. USA, *95:* 8795–800, 1998.
37. Mori, A., Arii, S., Furutani, M., Mizumoto, M., Uchida, S., Furuyama, H., Kondo, Y., Gorrin-Rivas, M. J., Furumoto, K., Kaneda, Y., and Imamura, M. Soluble Flt-1 gene therapy for peritoneal metastases using HVJ-cationic liposomes. Gene Ther., *7:* 1027–1033, 2000.
38. Yoneda, J., Kuniyasu, H., Crispens, M. A., Price, J. E., Bucana, C. D., and Fidler, I. J. Expression of angiogenesis-related genes and progression of human ovarian carcinomas in nude mice. J. Natl. Cancer Inst., *90:* 447–454, 1998.
39. Chen, C. A., Cheng, W. F., Lee, C. N., Chen, T. M., Kung, C. C., Hsieh, F. J., and Hsieh, C. Y. Serum vascular endothelial growth factor in epithelial ovarian neoplasms: correlation with patient survival. Gynecol. Oncol., *74:* 235–240, 1999.
40. Maass, G., Bogedain, C., Scheer, U., Michl, D., Horer, M., Braun-Falco, M., Volkenandt, M., Schadendorf, D., Wendtner, C. M., Winnacker, E. L., Kotin, R. M., and Hallek, M. Recombinant adeno-associated virus for the generation of autologous, gene-modified tumor vaccines: evidence for a high transduction efficiency into primary epithelial cancer cells. Hum. Gene Ther., *9:* 1049–1059, 1998.
41. Fisher, K. J., Jooss, K., Alston, J., Yang, Y., Haecker, S. E., High, K., Pathak, R., Raper, S. E., and Wilson, J. M. Recombinant adeno-associated virus for muscle directed gene therapy. Nat. Med., *3:* 306–312, 1997.
42. Russell, D. W., Miller, A. D., and Alexander, I. E. Adeno-associated virus vectors preferentially transduce cells in S phase. Proc. Natl. Acad. Sci. USA, *91:* 8915–8919, 1994.
43. Xiao, X., Li, J., and Samulski, R. J. Efficient long-term gene transfer into muscle tissue of immunocompetent mice by adeno-associated virus vector. J. Virol., *70:* 8098–108, 1996.

ELSEVIER

Cardiovascular Research 53 (2002) 993–1001

Cardiovascular Research

www.elsevier.com/locate/cardiores

AAV-mediated VEGF gene transfer into skeletal muscle stimulates angiogenesis and improves blood flow in a rat hindlimb ischemia model

Masahisa Shimpo[a,b], Uichi Ikeda[a,*], Yoshikazu Maeda[a], Masafumi Takahashi[a], Hiroshi Miyashita[a], Hiroaki Mizukami[b], Masashi Urabe[b], Akihiro Kume[b], Toshihiro Takizawa[c], Masabumi Shibuya[d], Keiya Ozawa[b], Kazuyuki Shimada[a]

[a]*Division of Cardiovascular Medicine, Jichi Medical School, Minamikawachi-Machi, Tochigi 329-0498, Japan*
[b]*Division of Genetic Therapeutics, Jichi Medical School, Minamikawachi-Machi, Tochigi 329-0498, Japan*
[c]*Department of Anatomy, Jichi Medical School, Minamikawachi-Machi, Tochigi 329-0498, Japan*
[d]*Department of Genetics, Institute of Medical Science, University of Tokyo, Tokyo, Japan*

Received 5 September 2001; accepted 12 November 2001

ELSEVIER

Cardiovascular Research 53 (2002) 993–1001

Cardiovascular Research

www.elsevier.com/locate/cardiores

AAV-mediated VEGF gene transfer into skeletal muscle stimulates angiogenesis and improves blood flow in a rat hindlimb ischemia model

Masahisa Shimpo[a,b], Uichi Ikeda[a,*], Yoshikazu Maeda[a], Masafumi Takahashi[a], Hiroshi Miyashita[a], Hiroaki Mizukami[b], Masashi Urabe[b], Akihiro Kume[b], Toshihiro Takizawa[c], Masabumi Shibuya[d], Keiya Ozawa[b], Kazuyuki Shimada[a]

[a]*Division of Cardiovascular Medicine, Jichi Medical School, Minamikawachi-Machi, Tochigi 329-0498, Japan*
[b]*Division of Genetic Therapeutics, Jichi Medical School, Minamikawachi-Machi, Tochigi 329-0498, Japan*
[c]*Department of Anatomy, Jichi Medical School, Minamikawachi-Machi, Tochigi 329-0498, Japan*
[d]*Department of Genetics, Institute of Medical Science, University of Tokyo, Tokyo, Japan*

Received 5 September 2001; accepted 12 November 2001

Abstract

Objectives: Clinical trials on therapeutic angiogenesis using vascular endothelial growth factor (VEGF) are ongoing, however the benefits of these therapies are still controversial. To establish a more efficient gene transfer method for ischemic diseases, we investigated the therapeutic potential of adeno-associated virus (AAV)-mediated VEGF gene transfer. **Methods:** We produced $VEGF_{165}$-expressing AAV vectors (AAV-VEGF). HEK-293 cells were transduced with AAV-VEGF in vitro and VEGF expression and secretion were examined. We used a rat ischemic hindlimb model and AAV-VEGF was administered intramuscularly into the ischemic limb. Gene expression was evaluated by RT-PCR and ELISA. Six weeks after gene transfer, we measured the blood flow of limb vessels and the skin temperature of limbs. Histochemical examination was performed to illustrate capillary growth. **Results:** Western blotting and ELISA revealed VEGF protein expression and secretion from AAV-VEGF-transduced HEK-293 cells. VEGF mRNA and protein expression was consistently observed in the injected muscle at least 10 weeks after the injection, while no VEGF mRNA could be detected at remote organs. The mean blood flow in AAV-VEGF-transduced ischemic limbs was significantly higher than in AAV-LacZ-transduced limbs. Capillary density was significantly higher in AAV-VEGF-injected tissues than in AAV-LacZ-injected tissues. **Conclusions:** This study demonstrates that (1) AAV-mediated VEGF gene transfer into rat skeletal muscles is efficient and stable without ectopic expression, and (2) AAV-mediated VEGF gene transfer stimulates angiogenesis and thereby improves blood flow in a rat hindlimb ischemia model. These findings suggest that AAV-mediated VEGF gene transfer may be useful for treatment of ischemic diseases.

Keywords: Angiogenesis; Atherosclerosis; Cytokines; Gene therapy; Growth factors; Ischemia

1. Introduction

Vascular endothelial growth factor (VEGF), also known as vascular permeability factor, is a heparin-binding dimeric glycoprotein and a principal angiogenic factor stimulating migration, proliferation, and expression of various genes in endothelial cells [1,2]. VEGF is synthesized by cells around the vasculature and affects endothelial cells as a paracrine factor. Its expression is upregulated by hypoxia and various cytokines. We previously reported increased circulating VEGF levels in patients with acute myocardial infarction [3]. VEGF has been shown to stimulate the development of collateral vessels in animal models of peripheral and myocardial ischemia [4–

*Corresponding author. Tel.: +81-285-58-7344; fax: +81-285-44-5317.
E-mail address: uikeda@jichi.ac.jp (U. Ikeda).

Time for primary review 27 days.

0008-6363/02/$ – see front matter
PII: S0008-6363(01)00546-6

6]. There are many patients with ischemic diseases for whom pharmacological intervention is ineffective and therapy is limited to surgical revascularization or endovascular interventional therapy. Promoting the formation of new collateral vessels in the ischemic myocardium and leg muscles is an important role for the treatment of such disorders. Recently, clinical trials of therapeutic angiogenesis using the VEGF gene have been initiated. Several uncontrolled clinical trials showed that VEGF gene transfer resulted in clinical improvement in patients with ischemic diseases [7,8]; however, the benefits of these therapies are still controversial [9].

Beneficial gene transfer vehicles are necessary for the clinical application of gene therapy. Recombinant viral vectors based on a non-pathogenic human parvovirus, adeno-associated virus (AAV), have a number of attractive features, including lack of cytotoxicity, ability to transduce both dividing and non-dividing cells [10], and long-term transgene expression [11–13]. AAV vectors can transduce efficiently to the skeletal muscles [13], cardiac myocytes [14,15], neurons [12,16,17], lungs [11], hepatocytes [18], renal cells [19], and endothelial cells [20], and have been evaluated in clinical trials for hemophilia B [21] and cystic fibrosis [22].

In the present study, in order to establish a more efficient and stable gene transfer method for ischemic diseases, we produced VEGF-expressing AAV vectors and assessed the efficiency and stability of AAV-mediated gene transfer into rat hindlimbs by intramuscular injection. Furthermore, we investigated whether AAV-mediated VEGF gene transfer could stimulate angiogenesis and thereby improve the hemodynamic deficit in the ischemic limb of a rat model.

2. Methods

2.1. Plasmid construction and vector production

The parent AAV vector plasmid pAAV-LacZ contains the LacZ reporter gene with the human cytomegalovirus (CMV) immediate early promoter and simian virus 40 polyadenylation signal sequence between the inverted terminal repeats (ITRs) of the AAV-2 genome [16]. The pAAV-VEGF vector plasmid was constructed by excising the LacZ reporter gene from the pAAV-LacZ and replacing it with the full-length human $VEGF_{165}$ cDNA isolated from the pUC18 vector [23].

We produced AAV vectors without the use of a helper adenovirus, as described previously [24]. The vector-production process involved cotransfection of human embryonic kidney cell line 293 (HEK-293) with the following plasmids: the AAV vector plasmid (pAAV-LacZ, pAAV-VEGF), the AAV helper plasmid, and the adenovirus helper plasmid, using the calcium phosphate method. Then, the AAV vectors were harvested and purified after two sequential continuous CsCl gradients as described [24]. The vector particle titer was determined by quantitative DNA dot-blot hybridization of DNase I-treated vector stocks.

2.2. In vitro transduction and Western blotting

HEK-293 cells were transduced with AAV vectors by adding the indicated amount of vector stock diluted in 10% fetal bovine serum (FBS) containing DMEM/F-12 medium for 24 h. Cells were rinsed with ice-cold phosphate-buffered saline (PBS) and resuspended in lysis buffer (1% Nonidit P-40, 50 mmol/l Tris–HCl, pH 7.4, 150 mmol/l NaCl, 200 U/ml aprotinine, 1 mmol/l PMSF). The cell lysates (10 μg of protein) were separated by 12% polyacrylamide gel electrophoresis and blotted onto polyvinylidene difluoride membranes. Immunoblotting was performed with anti-human VEGF antibody (Sigma, St. Louis, MO, USA) and the specific binding of the antibody was visualized with an ECL detection system (Amersham, UK).

2.3. Assay for VEGF concentration

HEK-293 cells were incubated with AAV-VEGF-containing medium for 24 h. Then, cells were washed with PBS twice and incubated in serum-free medium. Twenty-four hours after replacement of the culture medium, VEGF concentrations of the culture supernatant were measured with an enzyme-linked immunosorbent assay (ELISA) method using the Biotrak human VEGF ELISA system (Amersham) according to the manufacturer's instructions. In brief, 50 μl of each sample was added to an anti-human VEGF precoated plate and incubated at room temperature for 2 h. The plate was washed three times, and then biotinylated antibody reagent was added to the plate and incubated for 1 h. After washing, streptavidin-HRP reagent was added and incubated for 1 h. Finally, substrate solution was added to the plate and the optical density at 450 nm was determined. The standard curve was linear from 15.6 to 1000 pg/ml of VEGF. VEGF levels of the serum were also determined using the same ELISA system.

2.4. Intramuscular administration of AAV vectors

All animal experiments were performed in accordance with the *Jichi Medical School Guide for Laboratory Animals*, 1993. Male Sprague–Dawley rats (200–250 g) were anesthetized with diethyl ether. A skin incision about 5 mm in length was made over the tibialis anterior muscle and the fascia identified. AAV vectors were diluted in 50 mM Hepes-buffered saline and carbon black was added (Pelikan ink, Günther Wagner) to allow tracing of the injection site. The vector suspension containing AAV-LacZ (1.0×10^{13} particles/200 μl) and AAV-VEGF (1.8×10^{13}

particles/200 μl) was injected with a 29-gauge needle into two different sites (100 μl/site) in the tibialis anterior muscle.

2.5. RT-PCR

Gene expression at the mRNA level was evaluated by reverse transcription-polymerase chain reaction (RT-PCR). Total cellular RNA of muscle tissues and remote tissues (brain, heart, liver, spleen, kidney, testes) was isolated using RNA STAT-60 (TET-TEST, Friendswood, TX, USA). Extracted RNA was treated with DNase I (Takara Shuzo, Tokyo, Japan) to eliminate DNA contamination. The synthesis of first-strand cDNA was performed under the conditions recommended in the ProSTAR First Strand RT-PCR Kit (Stratagene, La Jolla, CA, USA). The PCR amplifications were performed using human VEGF specific primers (sense, 5′-GAGGGCAGAATCATCACGAAGT; antisense, 5′-TGAGAGATCTGGTTCCCGAAAC-3′) and glyceraldehyde 3-phosphate dehydrogenase (GAPDH) primers (sense, 5′-TATTGGGCGCCTGGTCACCA-3′; antisense, 5′-CCACCTTCTTGATGTCATCA-3′). GAPDH mRNA served as an internal standard. The PCR products were electrophoresed on ethidium bromide-stained 2.0% agarose gels.

2.6. Rat hindlimb ischemia model and gene transfer

Male Sprague–Dawley rats (200–250 g) were anesthetized with an intraperitoneal injection of sodium pentobarbital (50 mg/kg). A longitudinal incision was made in the right thigh, after which the right femoral artery was surgically excised to induce limb ischemia. Rats were then transduced with AAV-VEGF (2.0×10^{13} particles; $n=8$) or AAV-LacZ (1.5×10^{13} particles; $n=8$) via an intramuscular injection. The vector suspension (100 μl/site) was injected into four different sites in the major thigh muscles (quadriceps and adductor). Three rats received sham operations for preliminary assessment of hemodynamic examination.

2.7. Blood flow measurement and thermography

Six weeks after gene transfer, each rat was re-anesthetized with an intraperitoneal injection of sodium pentobarbital (50 mg/kg) and the lower body coats were shaved. The skin temperature of the rat hindlimb was measured with infrared thermography (TH3106ME, NEC San-ei Instruments, Tokyo, Japan).

Blood flow at the tibialis posterior artery was measured by a transit-time ultrasound flowmeter (T206, Transonic Systems, Ithaca, NY, USA) using a perivascular flowprobe. The tibialis posterior artery was dissected free and perivascular flowprobes placed according to the manufacturer's instructions. Blood flow of both the ischemic and contralateral limbs was recorded simultaneously, and was expressed as a percentage of the contralateral limbs.

2.8. Histological assessment

Muscle tissues were obtained as transverse sections from the quadriceps and adductor muscles of the ischemic limb after hemodynamic examination. Frozen sections were stained for alkaline phosphatase using an indoxyl-tetrazolium method to detect capillary endothelial cells, as described previously [25]. Capillary density was evaluated by histological examination of five randomly selected fields of one muscle section, and the number of capillaries was counted (mean number of capillary per square millimeter).

2.9. Statistical analysis

Results are expressed as mean±S.E.M. Statistical significance was evaluated by unpaired Student's t-test for comparisons between two means, and one-way ANOVA combined with Fisher's PLSD test for more than two means. A value of $P<0.05$ was considered statistically significant.

3. Results

3.1. AAV-mediated VEGF gene transfer in vitro

We initially performed in vitro transduction of the human $VEGF_{165}$ gene by AAV vectors. HEK-293 cells were incubated in a medium containing AAV-VEGF (1.0×10^5 particles/cell) for 24 h, and subjected to Western blotting. Immunoblotting using anti-human VEGF anti-

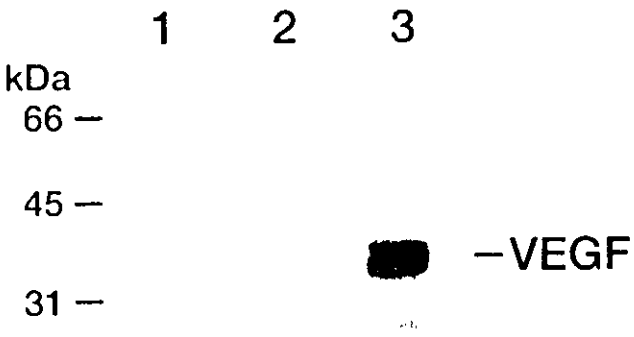

Fig. 1. Expression of human $VEGF_{165}$ protein in HEK-293 cells. HEK-293 cells were transduced with AAV-VEGF or AAV-LacZ and lysed 24 h after transduction. The VEGF protein was separated by 12% polyacrylamide gel electrophoresis and blotted onto a membrane. 42 kDa VEGF protein was evident in VEGF-transduced HEK-293 cells (lane 3), while no VEGF protein was expressed in both untransduced (lane 1) and LacZ-transduced (lane 2) HEK-293 cells.

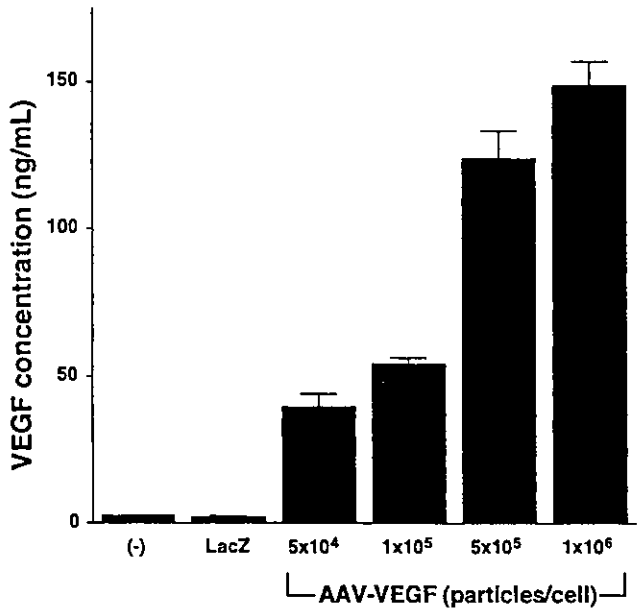

Fig. 2. VEGF concentrations in the culture supernatant of AAV-transduced HEK-293 cells. HEK-293 cells were exposed to increasing titers of AAV-VEGF or AAV-LacZ for 24 h. Then, 24 h after replacement of the culture medium, the VEGF concentration was measured by ELISA. The VEGF concentration is shown as the mean value±S.E.M. of measurements from one experiment ($n=4$), representative of three different experiments.

bodies clearly demonstrated 42 kDa VEGF protein expression in the VEGF-transduced HEK-293 cells (Fig. 1).

We next investigated whether VEGF was successfully released from the transduced HEK-293 cells. Cells were incubated with the vector-containing medium for 24 h, and the concentration of VEGF in the cultured medium was measured by ELISA. Fig. 2 demonstrates the relationship between AAV-VEGF vector concentrations and VEGF levels in the culture supernatant. VEGF levels in the culture supernatant increased in a titer-dependent manner (5×10^4–1×10^6 particles/cell). Conversely, the culture supernatant from non-transduced cells and LacZ-transduced cells contained quite low levels of VEGF.

3.2. VEGF gene transfer into skeletal muscles

We next performed in vivo gene transfer into the rat skeletal muscle using AAV vectors. To determine whether an AAV vector could be used to efficiently and stably transduce rat muscle tissues, 1.0×10^{13} particles of AAV-LacZ were injected into the tibialis anterior muscle. X-gal histochemical staining revealed efficient β-galactosidase expression (the majority of muscle fibers in the area of injection) at least 12 weeks after injection (data not shown). We then performed in vivo transduction of the human $VEGF_{165}$ gene by AAV vectors (1.8×10^{13} particles/site). To confirm human $VEGF_{165}$ gene expression in transduced rat tibialis anterior muscles, RT-PCR using human VEGF-specific primers was performed. VEGF gene expression was consistently observed 4 and 10 weeks after injections (Fig. 3). On the other hand, no gene expression was observed in AAV-LacZ-injected tibialis anterior muscles. No human $VEGF_{165}$ mRNA could be detected by RT-PCR from remote organs (brain, heart, liver, spleen, kidney, and testes) in AAV-VEGF-treated rats 4 weeks after injection (Fig. 3).

We further examined VEGF secretion from transduced muscle tissues. AAV vector-injected tibialis anterior muscle tissues were excised and cultured in serum-free DMEM/F-12 medium, and the VEGF concentrations of the culture supernatant were measured by ELISA. Ten weeks after gene transfer, significant amounts of VEGF (up to 5.3±1.5 ng/g tissue/24 h) were detected in the culture supernatant

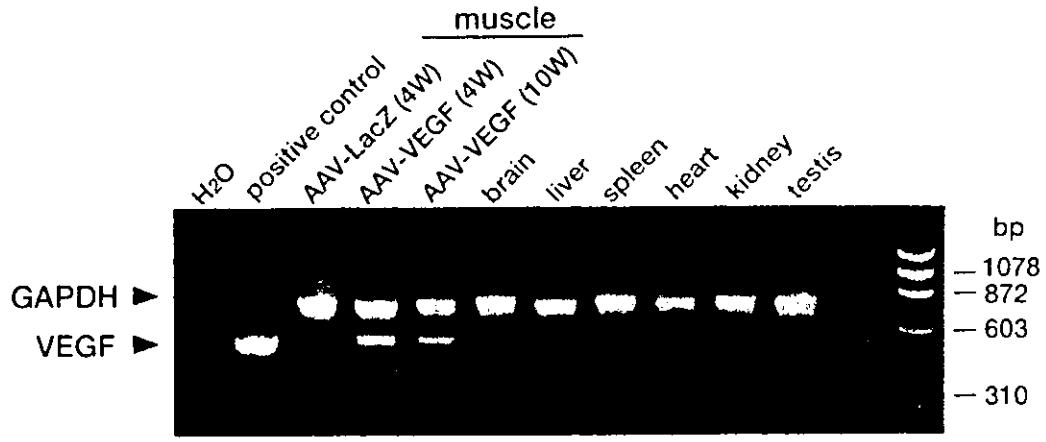

Fig. 3. Expression of VEGF mRNA in vector-injected muscle tissues and remote organs. Muscle tissues and other organs were isolated at 4 and 10 weeks after intramuscular injection and total RNA was extracted. After DNase-I treatment, RT-PCR using human VEGF-specific primers was performed. The sizes of PCR products for rat GAPDH and human VEGF were 747 and 531 bp, respectively. VEGF expression plasmid (pCMV-VEGF, 1 ng) was used as a positive control. GAPDH mRNA served as an internal standard. The PCR products were electrophoresed on ethidium bromide-stained 2.0% agarose gels. Three independent experiments yielded identical results.

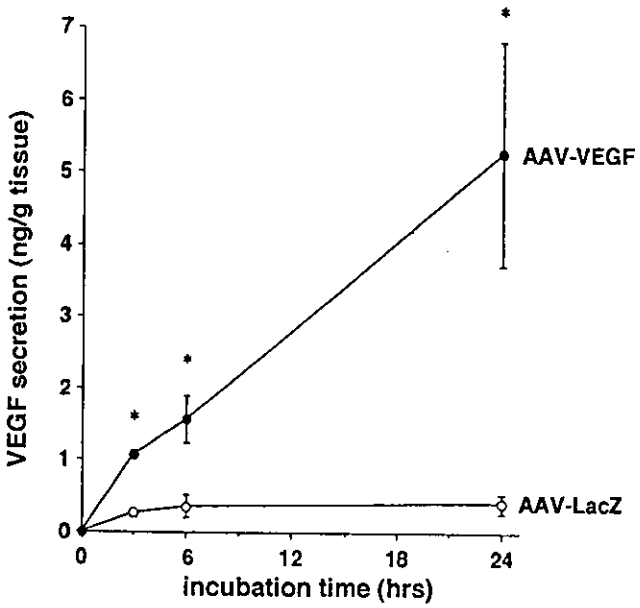

Fig. 4. VEGF secretion from AAV vector-injected tibialis anterior muscles. Ten weeks after gene transfer, muscle tissues were excised and cultured in serum-free DMEM/F-12 medium at 37 °C. After incubation for various periods as indicated on the X-axis, the VEGF concentration of the culture supernatant was measured by ELISA. VEGF concentrations were normalized to the protein content per dish and are shown as mean values±S.E.M. of measurements from one experiment ($n=4$), representative of two different experiments. *$P<0.05$ compared with values of AAV-LacZ-transduced muscles.

of AAV-VEGF-injected (1.8×10^{13} particles/site) muscle tissues (Fig. 4), while no substantial amount of VEGF was detected in AAV-LacZ-injected tissues. These results suggest constitutive expression and release of VEGF from AAV-VEGF-transduced muscles.

3.3. VEGF levels in the systemic circulation

Blood samples were also obtained from the peripheral veins of rats 1, 2, 4, and 8 weeks after AAV-VEGF transduction and analyzed with ELISA for human VEGF to detect VEGF levels in the systemic circulation. Serum VEGF levels were lower than the detectable level of the assay kit (15.6 pg/ml) at each time point.

3.4. VEGF gene transfer to a rat hindlimb ischemia model

We next investigated the therapeutic effects of AAV-mediated VEGF gene transfer. We performed AAV-mediated gene transfer by intramuscular injection into rat ischemic hindlimbs. Six weeks after gene transfer, we assessed the blood flow of rat hindlimbs using an ultrasound flowmeter. As shown in Fig. 5, the mean blood flow

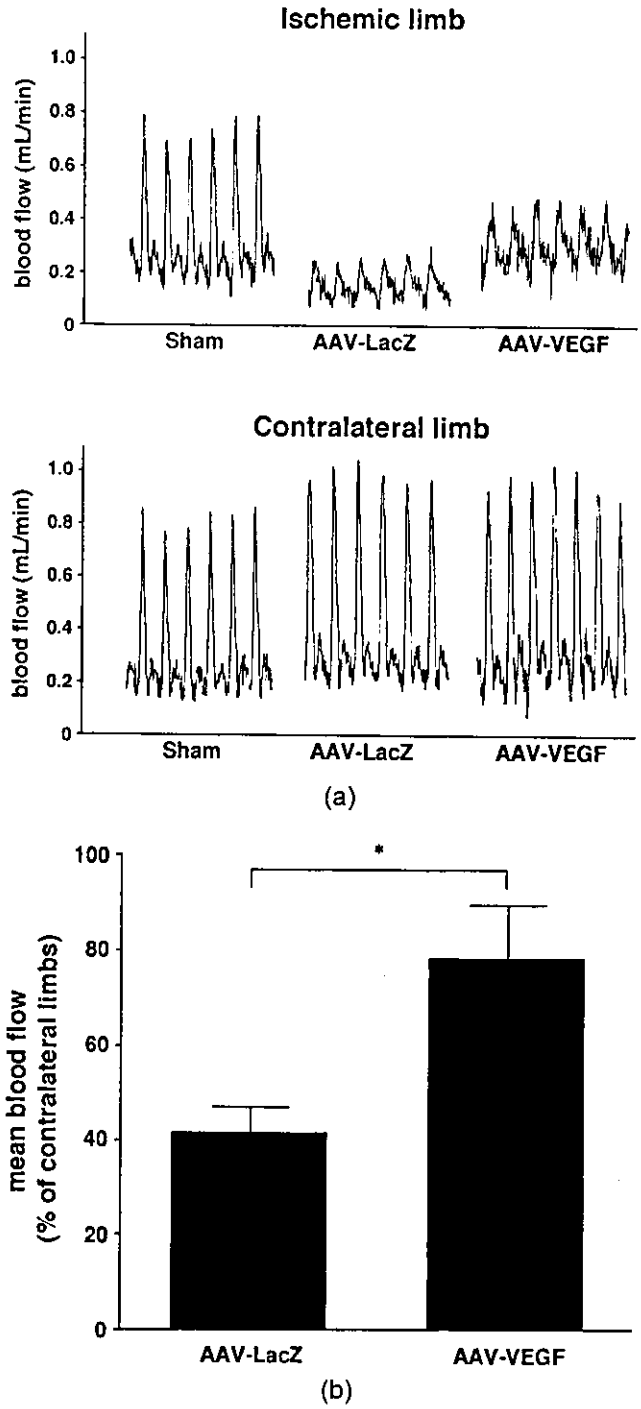

Fig. 5. Blood flow in the rat hindlimb was measured by a transit-time ultrasound flowmeter 6 weeks after gene transfer. After anesthetization, blood flow of both ischemic and contralateral limbs was recorded simultaneously in sham-operated ($n=3$), AAV-LacZ-transduced (1.5×10^{13} particles/body; $n=8$) and AAV-VEGF-transduced (2.0×10^{13} particles/body; $n=8$) rats. (A) Representative record of blood flow. (B) Mean blood flow in the ischemic limbs. Values are expressed as a percentage of contralateral limbs and are shown as mean values±S.E.M. *$P<0.01$.

in AAV-VEGF-transduced ischemic limbs (78.2±11.3% of contralateral limbs) was significantly higher than that in AAV-LacZ-transduced ischemic limbs (41.5±5.4%).

To assess the improved perfusion of ischemic limbs, we measured the skin temperature of the rat hindlimbs with infrared thermography. The skin temperature of the LacZ-transduced ischemic limb was about 2 °C lower than that of the contralateral limb. Conversely, AAV-mediated VEGF gene transfer brought about a restoration of the skin temperature in the ischemic limb (Fig. 6).

The thigh muscles of the ischemic limb were examined histologically 6 weeks after gene transfer. As shown in

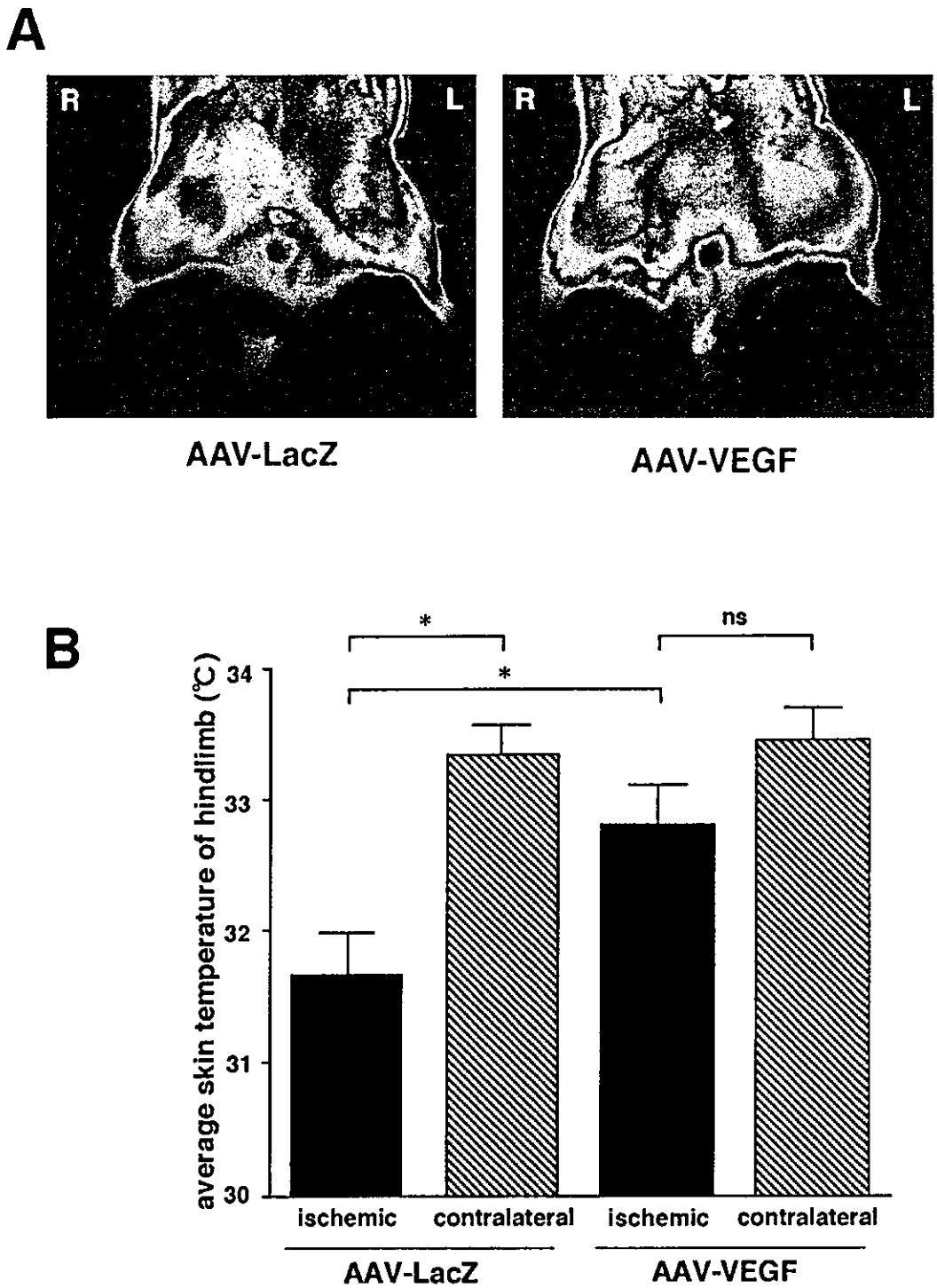

Fig. 6. Thermography of rat hindlimbs was performed 6 weeks after gene transfer. Rats were anesthetized and their lower body coats were shaved. The skin temperature of each rat hindlimb was measured with infrared thermography. (A) Color images of infrared thermography. R, ischemic limbs; L, contralateral limbs. (B) Average skin temperature (°C) of ischemic and contralateral hindlimbs in AAV-LacZ- (1.5×10^{13} particles/body; $n=4$) or AAV-VEGF- (2.0×10^{13} particles/body; $n=4$) transduced rats. *$P<0.05$.

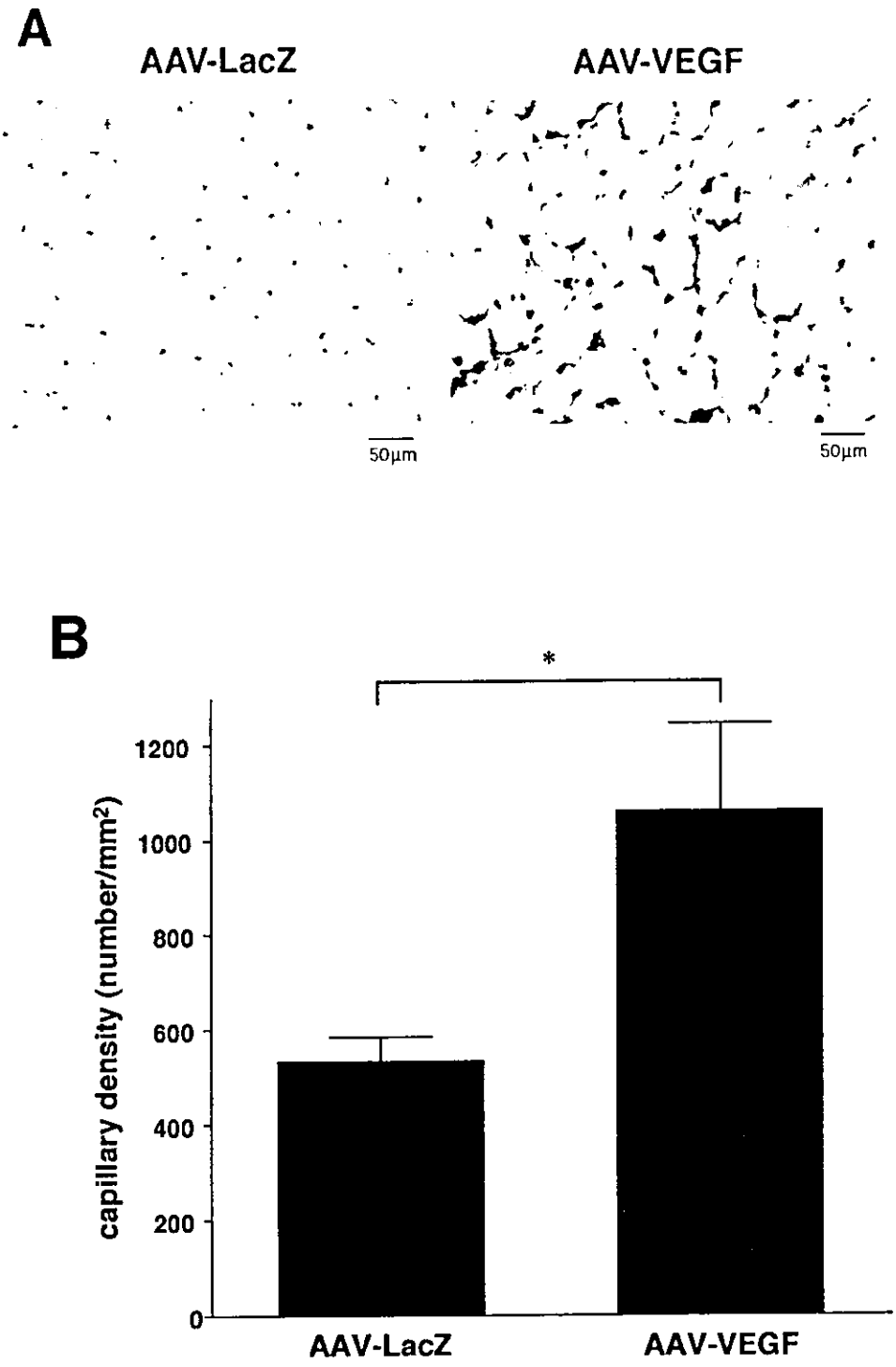

Fig. 7. (A) Representative images of rat muscle tissues using histochemical staining for alkaline phosphatase. (B) Capillary density in rat muscle tissues. Muscle tissues were obtained from the ischemic limbs of AAV-LacZ-transduced ($n=4$) and AAV-VEGF-transduced ($n=4$) rats. The number of capillaries was counted in five different fields of one muscle section, and capillary density was calculated. Data are shown as mean values±S.E.M. *$P<0.001$.

Fig. 7, capillary density was significantly higher in AAV-VEGF-injected muscle tissues (1062±75/mm^2) than that in AAV-LacZ-injected muscle tissues (532±24/mm^2). There was no angioma-like structure or inflammatory-cell infiltration observed in either ischemic or contralateral limbs.

4. Discussion

The present study was designed to examine whether the AAV vector is able to transfer the VEGF gene efficiently and safely. In the in vitro study, we revealed that AAV-mediated VEGF gene transfer into HEK-293 cells induced

the expression and secretion of VEGF. We also demonstrated that significant amounts of VEGF were detected in the culture supernatant of AAV-VEGF-injected muscle tissues, suggesting constitutive expression and release of VEGF from the muscle in vivo. However, serum VEGF levels in the systemic circulation were lower than the detectable level at each time point. This may be due to the very short biological half-life of VEGF; it may be secreted and function only in the local area of injection. Furthermore, no evidence of human $VEGF_{165}$ mRNA expression was observed at remote organs (brain, heart, liver, spleen, kidney, and testes) in AAV-VEGF-treated rats. These findings suggest that AAV-mediated gene transfer is safe without ectopic expression for administration of VEGF.

For therapeutic angiogenesis, several different strategies have been examined to deliver VEGF in animal models. In some cases, the recombinant protein was tested. In others, VEGF gene transfer using naked DNA or adenoviral vectors was performed. The use of naked DNA is simple and well tolerated by the recipient organism due to the low toxicity and immune response. However, the transduction efficiency is significantly lower compared with other methods. The adenovirus has frequently been the vector of choice for gene transfer because it is able to transduce a variety of cells with high efficiency. However, the major limitations of adenoviral vectors are lack of sustained expression, antigenicity against viral proteins by both humoral and cytotoxic T-lymphocytes, and possible toxicity at high doses. Recently, clinical trials on therapeutic angiogenesis using VEGF have been initiated. Arterial or intramuscular gene transfer of naked DNA encoding $VEGF_{165}$ in patients with severe limb ischemia produced angiographic and histological evidence of angiogenesis [7,26]. Clinical trials using naked VEGF DNA or adenovirus-mediated gene transfer in severe myocardial ischemia patients are also now ongoing [8,27]. However, a placebo-controlled phase II study, in which recombinant $VEGF_{165}$ was delivered as a single intracoronary infusion, followed by three intravenous infusions, did not demonstrate any clinical benefit [9], possibly due to short-term, transient expression of VEGF with that transfer method.

On the other hand, AAV vectors have a number of attractive features, including lack of cytotoxicity, ability to transduce both dividing and non-dividing cells [10], and longer-term transgene expression compared with plasmid or adenovirus-based methods [11–13,28]. In the present study, VEGF expression in rat skeletal muscles persisted for at least 10 weeks after AAV-mediated gene transfer without inflammatory response. We also demonstrated that AAV-mediated VEGF gene transfer promoted capillary growth in the ischemic limb. Furthermore, we clarified that the mean blood flow in VEGF-transduced ischemic limbs was significantly higher than that in LacZ-transduced limbs, and that the average skin temperature of the former was significantly higher than that of the latter. These findings showed that AAV-mediated VEGF gene transfer had therapeutic effects in a rat hindlimb ischemia model.

The formation of hemangioma is a considerable problem associated with prolonged and high-level expression of VEGF. Springer et al. [29] reported that high levels of serum VEGF (200 μg/ml) caused hemangiomas in skeletal muscles and that low serum levels (30 μg/ml) did not cause vascular malformations, but were sufficient to induce angiogenesis in ischemic muscles. It was also shown that retroviral vector-mediated VEGF gene transfer to murine hearts induced hemangioma formation [30]. At the vector dose we used, AAV-VEGF could induce angiogenesis in the local ischemic environment; however, there was no angioma-like structure observed in any of the ischemic or contralateral limbs. Very recently, Byun et al. [31] reported AAV-mediated VEGF transfer into a rat hindlimb ischemia model. Regional blood flow and capillary density were significantly increased with an increase in tissue VEGF mRNA levels, but there was no detectable increase in serum VEGF levels. Su et al. [32] reported AAV-mediated VEGF gene transfer into the mouse ischemic heart. AAV-mediated VEGF transfer induced angiogenesis in the ischemic heart. There was no angioma observed in the heart and no VEGF was detected in the mouse serum. These and our findings suggest that AAV-mediated VEGF expression is not as high as those mediated by adenoviral and retroviral vectors, yet it is sufficient to induce new vascular formation in ischemic tissue. Thus, with an appropriate dose, AAV may represent the ideal vector for VEGF delivery.

In summary, the present study demonstrated that AAV-mediated gene transfer into rat skeletal muscles caused efficient and stable gene expression without ectopic expression. We also demonstrated that AAV-mediated VEGF gene transfer stimulates angiogenesis and thereby improves blood flow in a rat hindlimb ischemia model. These findings suggest that AAV-mediated VEGF gene transfer may be useful in the treatment of ischemic diseases.

Acknowledgements

We thank Avigen Inc. (Alameda, CA) for providing the AAV vector production system. This study was supported by the Ministry of Education, Culture, Sports, Science and Technology, and the Ministry of Health, Labour and Welfare, Japan.

References

[1] Leung DW, Cachianes G, Kuang WJ, Goeddel DV, Ferrara N. Vascular endothelial growth factor is a secreted angiogenic mitogen. Science 1989;246:1306–1309.

[2] Ferrara N, Houck K, Jakeman L, Leung DW. Molecular and biological properties of the vascular endothelial growth factor family of proteins. Endocr Rev 1992;13:18–32.

[3] Hojo Y, Ikeda U, Zhu Y et al. Expression of vascular endothelial growth factor in patients with acute myocardial infarction. J Am Coll Cardiol 2000;35:968–973.

[4] Takeshita S, Zheng LP, Brogi E et al. Therapeutic angiogenesis. A single intraarterial bolus of vascular endothelial growth factor augments revascularization in a rabbit ischemic hind limb model. J Clin Invest 1994;93:662–670.
[5] Hariawala MD, Horowitz JJ, Esakof D et al. VEGF improves myocardial blood flow but produces EDRF-mediated hypotension in porcine hearts. J Surg Res 1996;63:77–82.
[6] Banai S, Jaklitsch MT, Shou M et al. Angiogenic-induced enhancement of collateral blood flow to ischemic myocardium by vascular endothelial growth factor in dogs. Circulation 1994;89:2183–2189.
[7] Baumgartner I, Pieczek A, Manor O et al. Constitutive expression of phVEGF165 after intramuscular gene transfer promotes collateral vessel development in patients with critical limb ischemia. Circulation 1998;97:1114–1123.
[8] Losordo DW, Vale PR, Symes JF et al. Gene therapy for myocardial angiogenesis: initial clinical results with direct myocardial injection of phVEGF165 as sole therapy for myocardial ischemia. Circulation 1998;98:2800–2804.
[9] Henry TD, Annex BH, Azrin MA et al. Double blind, placebo controlled trial of recombinant human vascular endothelial growth factor—The VIVA Trial. J Am Coll Cardiol 1999;33:384A.
[10] Flotte TR, Afione SA, Zeitlin PL. Adeno-associated virus vector gene expression occurs in nondividing cells in the absence of vector DNA integration. Am J Respir Cell Mol Biol 1994;11:517–521.
[11] Flotte TR, Afione SA, Conrad C et al. Stable in vivo expression of the cystic fibrosis transmembrane conductance regulator with an adeno-associated virus vector. Proc Natl Acad Sci USA 1993;90:10613–10617.
[12] Kaplitt MG, Leone P, Samulski RJ et al. Long-term gene expression and phenotypic correction using adeno-associated virus vectors in the mammalian brain. Nat Genet 1994;8:148–154.
[13] Kessler PD, Podsakoff GM, Chen X et al. Gene delivery to skeletal muscle results in sustained expression and systemic delivery of a therapeutic protein. Proc Natl Acad Sci USA 1996;93:14082–14087.
[14] Maeda Y, Ikeda U, Shimpo M et al. Efficient gene transfer into cardiac myocytes using adeno-associated virus (AAV) vectors. J Mol Cell Cardiol 1998;30:1341–1348.
[15] Svensson EC, Marshall DJ, Woodard K et al. Efficient and stable transduction of cardiomyocytes after intramyocardial injection or intracoronary perfusion with recombinant adeno-associated virus vectors. Circulation 1999;99:201–205.
[16] Fan DS, Ogawa M, Fujimoto KI et al. Behavioral recovery in 6-hydroxydopamine-lesioned rats by cotransduction of striatum with tyrosine hydroxylase and aromatic L-amino acid decarboxylase genes using two separate adeno-associated virus vectors. Hum Gene Ther 1998;9:2527–2535.
[17] Fan DS, Ogawa M, Ikeguchi K et al. Prevention of dopaminergic neuron death by adeno-associated virus vector-mediated GDNF gene transfer in rat mesencephalic cells in vitro. Neurosci Lett 1998;248:61–64.
[18] Koeberl DD, Alexander IE, Halbert CL, Russell DW, Miller AD. Persistent expression of human clotting factor IX from mouse liver after intravenous injection of adeno-associated virus vectors. Proc Natl Acad Sci USA 1997;94:1426–1431.
[19] Shimpo M, Ikeda U, Maeda Y et al. Gene transfer into rat renal cells using adeno-associated virus vectors. Am J Nephrol 2000;20:242–247.
[20] Maeda Y, Ikeda U, Ogasawara Y et al. Gene transfer into vascular cells using adeno-associated virus (AAV) vectors. Cardiovasc Res 1997;35:514–521.
[21] Kay MA, Manno CS, Ragni MV et al. Evidence for gene transfer and expression of factor IX in haemophilia B patients treated with an AAV vector. Nat Genet 2000;24:257–261.
[22] Flotte T, Carter B, Conrad C et al. A phase I study of an adeno-associated virus-CFTR gene vector in adult CF patients with mild lung disease. Hum Gene Ther 1996;7:1145–1159.
[23] Sawano A, Takahashi T, Yamaguchi S, Aonuma M, Shibuya M. Flt-1 but not KDR/Flk-1 tyrosine kinase is a receptor for placenta growth factor, which is related to vascular endothelial growth factor. Cell Growth Differ 1996;7:213–221.
[24] Matsushita T, Elliger S, Elliger C et al. Adeno-associated virus vectors can be efficiently produced without helper virus. Gene Ther 1998;5:938–945.
[25] Ziada AM, Hudlicka O, Tyler KR, Wright AJ. The effect of long-term vasodilatation on capillary growth and performance in rabbit heart and skeletal muscle. Cardiovasc Res 1984;18:724–732.
[26] Isner JM, Pieczek A, Schainfeld R et al. Clinical evidence of angiogenesis after arterial gene transfer of phVEGF165 in patient with ischaemic limb. Lancet 1996;348:370–374.
[27] Rosengart TK, Lee LY, Patel SR et al. Angiogenesis gene therapy: phase I assessment of direct intramyocardial administration of an adenovirus vector expressing VEGF121 cDNA to individuals with clinically significant severe coronary artery disease. Circulation 1999;100:468–474.
[28] Coe S, Harron M, Winslet M, Goldspink G. The use of skeletal muscle to express genes for the treatment of cancer. Adv Exp Med Biol 2000;465:95–111.
[29] Springer ML, Chen AS, Kraft PE, Bednarski M, Blau HM. VEGF gene delivery to muscle: potential role for vasculogenesis in adults. Mol Cell 1998;2:549–558.
[30] Lee RJ, Springer ML, Blanco-Bose WE et al. VEGF gene delivery to myocardium: deleterious effects of unregulated expression. Circulation 2000;102:898–901.
[31] Byun J, Heard JM, Huh JE et al. Efficient expression of the vascular endothelial growth factor gene in vitro and in vivo, using an adeno-associated virus vector. J Mol Cell Cardiol 2001;33:295–305.
[32] Su H, Lu R, Kan YW. Adeno-associated viral vector-mediated vascular endothelial growth factor gene transfer induces neovascular formation in ischemic heart. Proc Natl Acad Sci USA 2000;97:13801–13806.

THE JOURNAL OF BIOLOGICAL CHEMISTRY
Vol. 277, No. 43, Issue of October 25, pp. 40768–40774, 2002
Printed in U.S.A.

Identification of ATF-2 as a Transcriptional Regulator for the Tyrosine Hydroxylase Gene*

Received for publication, June 18, 2002, and in revised form, August 7, 2002
Published, JBC Papers in Press, August 23, 2002, DOI 10.1074/jbc.M206043200

Takahiro Suzuki‡, Tohru Yamakuni§¶, Masatoshi Hagiwara‖, and Hiroshi Ichinose‡**

From the ‡Division of Molecular Genetics, Institute for Comprehensive Medical Science, Fujita Health University, Toyoake, Aichi 470-1192, Japan, the §Department of Pharmaceutical Molecular Biology, Graduate School of Pharmaceutical Sciences, Tohoku University, Aoba, Aramaki, Aoba-ku, Sendai 980-8578, Japan, the ¶Mitsubishi Kagaku Institute of Life Sciences, 11 Minamiooya, Machida, Tokyo 194-8511, Japan, and the ‖Department of Functional Genomics, Medical Research Institute, Tokyo Medical and Dental University, Tokyo 113-8510, Japan

Transcriptional regulation of catecholamine-synthesizing genes is important for the determination of neurotransmitters during brain development. We found that three catecholamine-synthesizing genes were transcriptionally up-regulated in cloned PC12D cells overexpressing V-1, a protein that is highly expressed during postnatal brain development (1). To reveal the molecular mechanism to regulate the expression of tyrosine hydroxylase (TH), which is the rate-limiting enzyme for catecholamine biosynthesis, we analyzed the transcription factors responsible for TH induction in the V-1 clonal cells. First, by using reporter constructs, we found that the transcription mediated by cAMP-responsive element (CRE) was selectively enhanced in the V-1 cells, and TH promoter activity was totally dependent on the CRE in the promoter region of the TH gene. Next, immunoblot analyses and a transactivation assay using a GAL4 reporter system revealed that ATF-2, but not cAMP-responsive element-binding protein (CREB), was highly phosphorylated and activated in the V-1 cells, while both CREB and ATF-2 were bound to the TH-CRE. Finally, the enhanced TH promoter activity was competitively attenuated by expression of a plasmid containing the ATF-2 transactivation domain. These data demonstrated that activation of ATF-2 resulted in the increased transcription of the TH gene and suggest that ATF-2 may be deeply involved in the transcriptional regulation of catecholamine-synthesizing genes during neural development.

Catecholamines are synthesized from L-tyrosine by the sequential action of four enzymes: tyrosine is converted to DOPA by tyrosine hydroxylase (TH),[1] DOPA to dopamine by aromatic L-amino acid decarboxylase (AADC), dopamine to norepinephrine by dopamine β-hydroxylase (DBH), and norepinephrine to epinephrine by phenylethanolamine *N*-methyltransferase. The regulation of the gene expression of these enzymes is important for the determination of the expression of neurotransmitters during brain development as well as for brain function under physiological and pathological conditions.

TH is the rate-limiting enzyme for catecholamine biosynthesis. The transcriptional regulation of the TH gene has been extensively studied, and many transcription factors were suggested to regulate TH gene expression. CREB, ATF-1, and CREM were shown to recognize the cAMP-responsive element (CRE) located at position −45/−38 in the TH promoter (2–6). CREB was reported to mediate basal and cAMP-induced TH transcription in various cultured cells including PC12 cells by the use of dominant-negative CREB protein and antisense RNA against CREB (7–10). CREB is activated by phosphorylation on Ser^{133} (11, 12). The activation of CREB by phosphorylation has been shown to mediate PKA-dependent (7, 13–15) and -independent (13, 14) induction of TH transcription. Functional and physiological roles of ATF-1 and CREM for TH transcription remained unclear. AP-1 transcription factors bound to the TPA-responsive element located at −205/−199 in the TH promoter, which also plays a critical role in the transcriptional induction of the TH gene (16). Expression of AP-1 family was induced by several stimuli to enhance TH gene transcription, and overexpression of Fra-2 and c-Fos stimulated TH transcription in PC12 and PC18 cells, respectively (17, 18).

Nurr1 and Ptx3/Pitx3, which are expressed in midbrain dopaminergic neuron at embryonic stage, were recently shown to regulate TH gene expression. Nurr1-null mice lacked TH immunoreactivity in midbrain (19), and overexpression of Nurr1 was shown to induce the TH gene expression in neural stem cells (20, 21). However, it is unclear whether or not Nurr1 directly acts on its responsive element in the TH promoter region (20, 21). Overepxression of Ptx3/Pitx3 activated the TH promoter activity in neuroblastoma cells through its responsive elements (22, 23).

Three of the catecholamine-synthesizing enzymes, *i.e.* TH, AADC, and DBH, were up-regulated in cloned PC12D cells overexpressing V-1 (1). V-1 is an adaptor-like protein, the expression of which is transiently high during postnatal brain development (24, 25). Therefore, V-1 potentially participate TH

* This work was supported by grants from the programs grants-in-aid for Encouragement of Young Scientists (to T. S.); grants-in-aid for Scientific Research on Priority Areas (C), Advanced Brain Science Project (to H. I.), from the Ministry of Education, Culture, Sports, Science, and Technology of Japan; Health Science Research Grants, Research on Human Genome, Tissue Engineering Food Biotechnology, from the Ministry of Health, Labor, and Welfare of Japan (to H. I.); and Human Frontier Science Program (to H. I.). The costs of publication of this article were defrayed in part by the payment of page charges. This article must therefore be hereby marked "*advertisement*" in accordance with 18 U.S.C. Section 1734 solely to indicate this fact.

** To whom correspondence should be addressed: Division of Molecular Genetics, Inst. for Comprehensive Medical Science, Fujita Health University, Toyoake, Aichi 470-1192, Japan. Tel.: 81-562-93-9391; Fax: 81-562-93-8831; E-mail: hichi@fujita-hu.ac.jp.

[1] The abbreviations used are: TH, tyrosine hydroxylase; AADC, aromatic L-amino acid decarboxylase; DBH, dopamine β-hydroxylase; CRE, cAMP-responsive element; CREB, cAMP-responsive element-binding protein; CREM, cAMP-responsive element modulator; PKA, protein kinase A; FSK, forskolin; NGF, nerve growth factor; GCH, GTP cyclohydrolase I; MEKK, mitogen-activated protein kinase/extracellular signal-regulated kinase kinase kinase.

gene expression in postnatal brain development. We were interested in the intracellular events in the V-1-overexpressing PC12D cells, because none of the transcription factors are known to induce these catecholamine-synthesizing genes simultaneously.

In the present study, we found that the transcription mediated by CRE was specifically and highly elevated in the V-1 cells, and that transcription of the TH gene is enhanced by activation of ATF-2, which directly acted on the CRE in the TH promoter. Our results suggest that ATF-2 is involved in the expression of the TH gene during neural development.

MATERIALS AND METHODS

Cell Culture—Two PC12D clones stably and highly expressing V-1, named V1-46 and V1-69, and two vector control clones, termed C-7 and C-9, were established as described previously (1). Parental PC12D cells were cultured in Dulbecco's modified Eagle's medium containing 10% horse serum and 5% fetal bovine serum. The stable clones were cultured in medium containing 280 μg/ml G418 (Invitrogen).

Reporter Plasmids—Mouse TH genomic DNA containing 5.5 kb of its 5′-flanking region, and exon 1 was originally isolated from a mouse genomic library and cloned into the pBluescript II KS(+) plasmid (mTH5.5-pBS). First, to produce mTHpro0.8-Luc, which contains the region of −752 bp from the transcriptional start site to the translational start site of the mouse TH gene, we amplified a fragment containing about 1.2 kb of the mouse TH 5′-flanking region by PCR using primers GTTCCCTTAGTGAGAGGACAC (forward) and GGAATTCCATGGTGCAAGCTGGTGGTC (reverse) and mTH5.5-pBS. The region between −752 bp from the transcriptional start position and the translational start site was ligated to a firefly luciferase reporter plasmid, PGV-B2 (Toyoink, Tokyo). The entire sequence of the inserted TH 5′-flanking region was confirmed by DNA sequencing using an ABI PRISM 310 genetic analyzer (Applied Biosystems). Next, to produce mTHpro4.3-Luc, a fragment that corresponded to the region between −4326 and −753 bp from the transcriptional start position was isolated by the digestion of mTH5.5-pBS with *Xho*I and then inserted into the *Xho*I site of mTHpro0.8-Luc. To produce a CRE mutant of mTHpro0.8-Luc that contained a 4-base deletion in a canonical CRE sequence of the TH promoter region (TGACGTCA), we digested the wild-type mTHpro0.8-Luc with *Aat*II to result in a plasmid cut in the middle of the CRE sequence, blunted the end with T4 exonuclease, and then religated it.

Firefly luciferase reporter plasmids containing a cyclic AMP-, AP-1-, NF-κB-, glucocorticoid-, heat shock protein-, or serum-responsive element upstream of a TATA-like promoter (P_{TAL}) region taken from herpes simplex thymidine kinase promoter were purchased from Clontech. The following plasmids were purchased from Stratagene as parts of PathDetect *trans*-reporting systems: pFC-MEKK and pFC-PKA are MEKK (amino acids 380 to 672) and PKA (catalytic subunit) expression vectors, respectively; pFA2-CREB and pFA-ATF-2 are expression vectors that consist of CREB (amino acids 1–280) and ATF-2 (amino acids 1–96) transactivation domains fused to the GAL4 DNA binding domain ($GAL4_{DBD}$, amino acids 1–147), respectively; pFC-dbd is the control vector for $GAL4_{DBD}$ only; and pFR-Luc reporter is a reporter plasmid containing five copies of the GAL4-responsive element.

DNA Transfection and Luciferase Assay—Seapansy luciferase vectors, pRL-CMV and pRL-TK (Toyoink), were used as an internal control to normalize for variations in transfection efficiency. Cells were transfected by lipofection using LipofectAMINE 2000 (Invitrogen). One day prior to transfection, the cells were plated on 24-well plates and transfected at ~50% confluence. In the experiments shown in Figs. 1–3, the cells were transfected with 0.75 μg of the firefly reporter plasmids and 0.05 μg of pRL-CMV per well. In experiments using the GAL4 system shown in Fig. 6, cells were transfected with 0.65 μg of pFR-Luc, 0.05 μg of pFA2-CREB or pFA-ATF-2, and 0.05 μg of pRL-TK per well. As a positive control, 0.05 μg of a PKA-expression vector (PKA) or a MEKK-expression vector (MEKK) was used for co-transfection of the parental PC12D cells, and otherwise, pBluescript plasmid was used as a carrier DNA. In the experiments shown in Fig. 7, the cells were transfected with 0.25 μg of mTHpro4.3-Luc or PGV-C2 (a SV40 promoter luciferase vector, Toyoink), 0.5 μg of pFA-ATF2, pFA2-CREB, or pFC2-dbd, and 0.05 μg of pRL-CMV per well. At 48 h after transfection, the cells were harvested and assayed for firefly and seapansy luciferase activities by using a PicaGene Dual luciferase assay kit (Toyoink).

Preparation of Cell Lysates—Cells were washed three times, suspended in ice-cold phosphate-buffered saline, and then pelleted in a microcentrifuge at 300 × *g* for 3 min. For preparation of nuclear extracts for electrophoretic mobility shift assays and immunoblot analysis of phosphorylated proteins, the cell pellet was lysed, and nuclear proteins were extracted as described (26) except that all buffers contained 0.10 volume of a Protease Inhibitors Cocktail (Sigma) substitute for phenylmethylsulfonyl fluoride and contained 0.01 volume of Phosphatase Inhibitor Cocktails I and II (Sigma). Protein concentration of the nuclear extract was determined by the method of Bradford (27), with bovine γ-globulin used as a standard. For preparation of whole-cell extracts for immunoblot analysis of phosphorylated proteins, the cell pellet was directly lysed in SDS-sample buffer, and the supernatant was collected as the whole-cell extract. The cell lysates were stored at −80 °C in small aliquots until assayed.

Electrophoretic Mobility Shift Assay—Sense and antisense strands of rat TH-CRE oligonucleotides (sense, GAGGGGCTTTGACGTCAGCCTGG) were annealed and end-labeled with [γ-^{32}P]ATP (6000 Ci/mmol, PerkinElmer Life Sciences) by use of T4 polynucleotide kinase. DNA-protein binding reactions were performed as described by Nankova *et al.* (18) with a slight modification. Briefly, the basic binding buffer contained 0.5 μg/μl bovine serum albumin, 0.1 μg/μl poly(dI-dC), 1 ng of end-labeled TH-CRE oligonucleotide (~35,000 cpm), and 10 μg of nuclear extract. Double-stranded oligonucleotides or antibodies (1 μl; Cell Signaling Technology) were preincubated on ice for 1 h prior to the addition of the labeled oligonucleotide, and the reaction was initiated by the addition of the labeled oligonucleotide. The mixture was then incubated for 20 min at room temperature. Electrophoresis was performed as described by Kapatos *et al.* (28), and radioactivity was visualized by exposing the x-ray film for 12 h at −80 °C.

Immunoblot Analysis—Phosphorylated form-specific and nonspecific antibodies against CREB, ATF-2, and c-Jun were purchased from Cell Signaling Technology. Immunoblotting were performed following the supplier's protocol. The cell lysate was separated by SDS-PAGE and transferred to a polyvinylidene difluoride membrane (Bio-Rad). Proteins were visualized with ECL plus (Amersham Biosciences).

Statistics—Student's *t* test was used for statistical evaluations. A level of $p < 0.05$ was accepted as statistically significant.

RESULTS

Increased Promoter Activity of the TH Gene in Clonal PC12D Cells Overexpressing V-1—We previously described that TH enzymatic activity, protein level, and mRNA level were all elevated in V-1-overexpressing clones (V1-46 and V1-69) compared with their values for the control (C-7 and C-9) clones (1). To examine the transcription of the TH gene in the V-1 and control clones, we transfected the cloned cells with plasmid constructs containing 4.3 kb of mouse TH 5′-flanking region fused to a luciferase reporter gene (mTHpro4.3-Luc). Reporter activity relative to pRL-CMV was significantly increased in the V-1 clones compared with that in the control clones (Fig. 1), suggesting that the increased level of TH mRNA in the V-1 clones was mainly due to an increased transcriptional rate and that *cis*-acting DNA elements located within the 4.3 kb of 5′-flanking region of the TH gene were required for the overexpression of the TH gene.

CRE-mediated Transcription Was Increased in the V-1 Clones—To explore the transcriptional events changed in the V-1 clones, we measured promoter activities of reporter genes containing cAMP-, AP-1-, NF-κB-, glucocorticoid-, heat shock protein-, and serum-responsive elements. In the V-1 clones, we found that the transcriptional activity mediated by CRE was greatly elevated compared with that in the control clones, whereas that mediated by the other elements was unchanged (Fig. 2).

Evaluation of CRE-dependent Expression of the TH Gene in the V-1 Clones—A CRE consensus motif (TCACGTCA) exists in the 5′-flanking region of the rat TH gene (29), and the sequence and its location (near the TATA-box) are highly conserved among rat, mouse, and man (30). It was earlier shown that the TH-CRE was essential for both basal and cyclic AMP-induced transcription of the TH gene in various cell lines, including PC12 cells (3, 31) and a subclone of PC12 (29). To evaluate the contribution of the increased activity of CRE-mediated transcription to the increased transcription of the TH gene in the

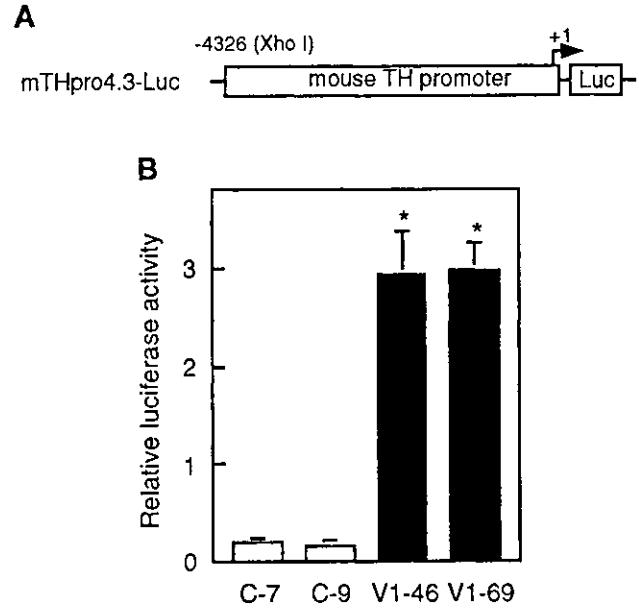

FIG. 1. **Transient transfection assay using a TH promoter construct.** *A*, diagram of a reporter plasmid containing 4.3 kb of the TH 5'-flanking region (mTHpro4.3-Luc). *B*, relative reporter activity of mTHpro4.3-Luc in V-1-overexpressing clones (V1-46 and V1-69; *closed bars*) and control clones (C-7 and C-9; *open bars*) was measured. A seapansy luciferase vector, pRL-CMV, was used as an internal control to normalize for variations in transfection efficiency. Data are the mean ± S.D. values from three independent experiments. Values of p were calculated from the two control clones, and the higher values are shown: *, $p < 0.05$.

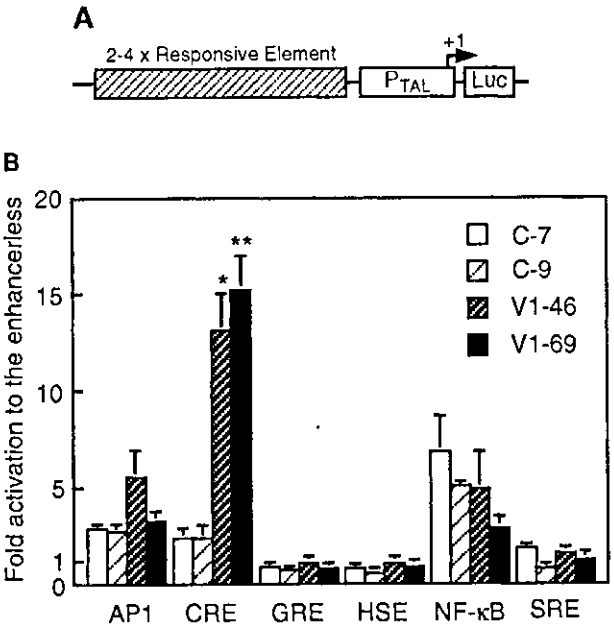

FIG. 2. **Enhancement of CRE-mediated transcription in the V-1 clones.** *A*, reporter vectors have a specific cis-acting element, cAMP-, AP-1-, NF-κB-, glucocorticoid-, heat shock protein-, or serum-responsive element (*AP1*, *CRE*, *GRE*, *HSE*, *κB*, and *SRE*, respectively), upstream from the TATA-like promoter region taken from the herpes simplex virus thymidine kinase (P_{TAL}) and connected to firefly luciferase cDNA. The control vector lacks the responsive element and has P_{TAL} only. *B*, The relative activity of the reporter gene in one clone was evaluated as -fold activation to the activity of the control vector in the same clone. Transfection efficiency was normalized using pRL-CMV. Data are the mean ± S.D. values from three to five independent experiments. Values of p for CRE activities of V-1 clones were calculated from the 2 control clones and the higher values are shown: *, $p < 0.05$; **, $p < 0.001$.

V-1 clonal cells, we made wild-type and CRE-mutagenized TH reporter vectors containing about 0.8 kb of the mouse TH 5'-flanking region upstream from the transcriptional start site (mTHpro0.8-Luc; Fig. 3*A*). The reporter activity of the wild-type mTHpro0.8-Luc was markedly increased in V1-69 cells (Fig. 3*B*), as had been the case for mTHpro4.3-Luc (Fig. 1). The reporter activity of the CRE mutant was almost the same as that of the promoter-less vector, PGV-B2 in V1-69, C-7, and the parental PC12D cells (Fig. 3*B*). Results for the other V-1 clone, V1-46, were similar to those for V1-69 (data not shown). These results indicated the importance of the CRE-mediated transcription for the regulation of the TH gene expression in the V-1 cells.

Identification of ATF-2 as a Transcription Factor Binding to TH-CRE in PC12D Cells—To identify transcriptional factors that might be involved in the CRE-mediated transcription of the TH gene, we conducted an electrophoretic mobility shift assay using nuclear extracts of PC12D cells and analyzed binding proteins that made a complex with the TH-CRE (Fig. 4). There were major bands (*Bands 1–3*) that disappeared in a dose-dependent manner by the addition of excess amounts of cold TH-CRE competitor (Fig. 4, *lanes 2–5*). However, an excess molar amount of TH-CRE mutant also decreased the amount of Band 3 to the same extent as did the TH-CRE wild type, whereas Bands 1 and 2 remained almost unaffected (Fig. 4, *lanes 6–8*), indicating that Bands 1 and 2 represented the protein-DNA complexes specific to the TH-CRE. An anti-CREB antibody supershifted Band 2 to Band B (Fig. 4, *lane 13*), and an anti-ATF-2 antibody supershifted Band 1 to Band A (Fig. 4, *lane 14*), indicating that Bands 1 and 2 represented complexes containing ATF-2 and CREB, respectively. Since ATF-2 was reported to bind to CRE as a homodimer or as a heterodimer with c-Jun (32–34), we examined whether c-Jun was contained in the TH-CRE complex. An anti-c-Jun antibody did not supershift Band 1 containing ATF-2 (Fig. 4, *lane 15*).

We also conducted an electrophoretic mobility shift assay using TH-CRE and nuclear extracts of V-1 and control clones. There was no significant difference in band patterns between V-1 or control clones and the parental PC12D cells (data not shown). These data suggest that proteins binding to the TH-CRE, including CREB and ATF-2, were not dramatically changed in the V-1 clones.

Activation of ATF-2 in the V-1 Clones—CREB and ATF-2 are well characterized among ATF/CRE binding proteins; phosphorylation of CREB on Ser^{133} (11, 12) or phosphorylation of ATF-2 on $Thr^{69/71}$ (35, 36) activates the CRE-mediated transcription. Since we identified CREB and ATF-2 as transcription factors binding to the TH-CRE as was shown in Fig. 4, we next examined the phosphorylation and expression of CREB and ATF-2 in the V-1 clones by Western blot analysis using phosphorylated form-specific and nonspecific antibodies against CREB or ATF-2. As positive controls, PC12D cells were treated with forskolin (FSK) or nerve growth factor (NGF) for 15 min (11, 37). In whole-cell extracts of FSK- or NGF-stimulated PC12D cells, the Ser^{133}-phosphorylated form of CREB was much increased (Fig. 5*A*, *upper panels*). Faster running bands that were immunostained with the antibody against CREB phosphorylated on Ser^{133} appeared, and the intensity of bands immunostained with anti-CREB antibody was reduced by FSK- and NGF-stimulation (Fig. 5*A*, *upper panels*), suggesting that CREB was rapidly degraded after its activation. In addition, phosphorylation of ATF-2 was also increased by FSK or NGF stimulation in PC12D cells, while the total amount of ATF-2 protein was unchanged (Fig. 5*A*, *lower panels*). In the V-1 clones, although there were no or few changes in the expression and phosphorylation of CREB compared with those in the control clones and the non-stimulated parental PC12D cells

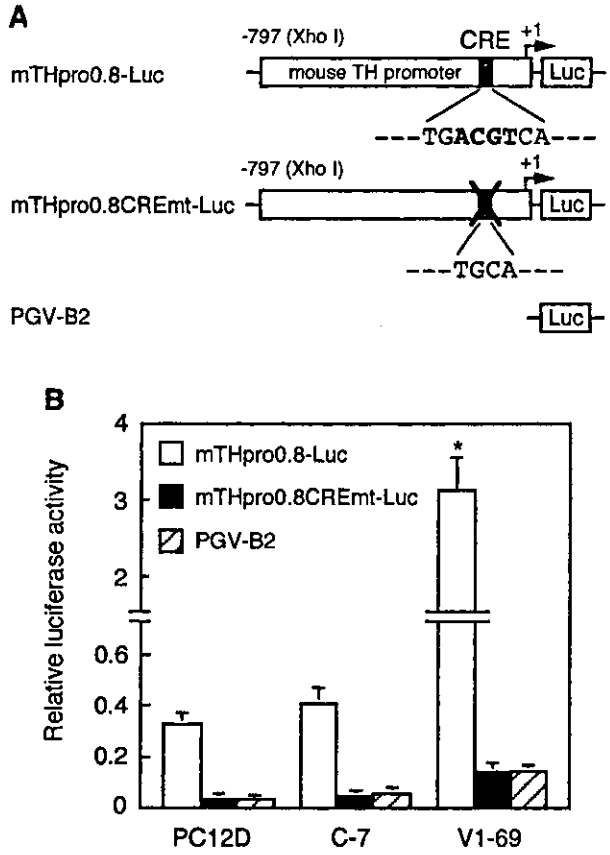

FIG. 3. **Deletion of CRE abolished transcription of a TH reporter gene in the V-1 and control cells.** *A*, reporter plasmids containing 0.8 kb of the TH 5′-flanking region without or with a mutation in the CRE consensus motif (mTHpro0.8-Luc and mTHpro0.8CREmt-Luc, respectively) were constructed. Deleted residues in the CRE mutant are in *boldface type*. *B*, reporter activities of the wild-type (*open bars*) and the CRE-mutant (*closed bars*) TH promoter constructs, and of the promoter-less vector PGV-B2 (*hatched bars*), were evaluated in a V-1 clone (V1-69) and in a control clone (C-7). Data are the mean ± S.D. values from three to six independent experiments. Values of p were calculated compared with the values of both the control clone and the parental PC12D cells: *, $p < 0.001$.

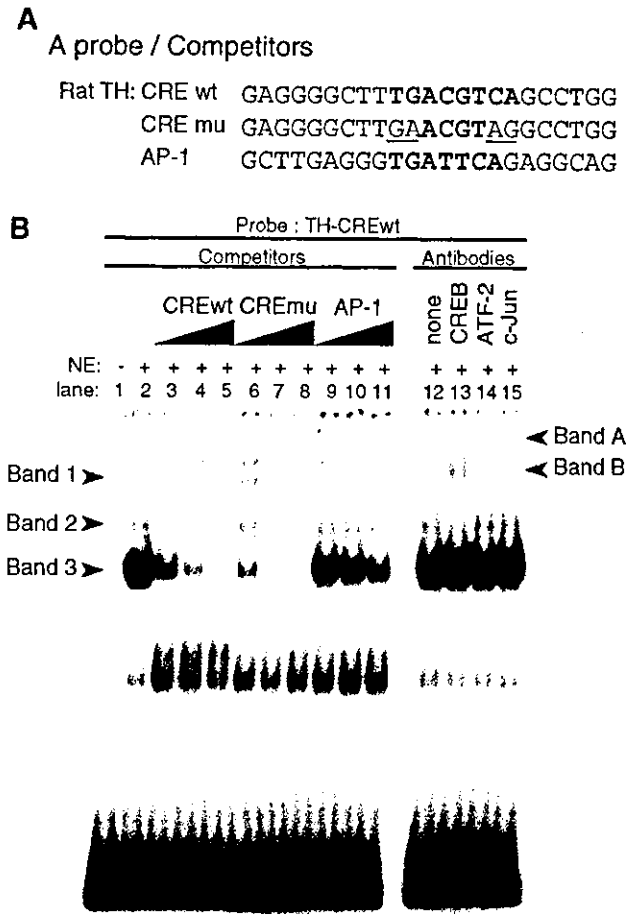

FIG. 4. **Analysis of DNA-protein complex formation between TH-CRE oligonucleotide and nuclear extract obtained from PC12D cells.** *A*, sequences of oligonucleotides used in this assay. Consensus sequences of CRE and AP-1 oligonucleotides (TH-CREwt and TH-AP-1) are in *boldface type*. Mutations in a CRE mutant oligonucleotide (TH-CREmu) are *underlined*. ^{32}P-Labeled TH-CREwt was used as a probe. Cold TH-CREwt, TH-CREmu, and TH-AP-1 were used in excess amount as competitors. *B*, binding of nuclear extract obtained from PC12D cells to ^{32}P-labeled TH-CREwt. Descriptions of lanes: *1*, free probe; *2–11*, competition assay with excess molar excess (10-, 30-, and 100-fold) of cold oligonucleotides; *12–15*, supershift assay with antibodies; *2*, buffer control for competitors; *3–5*, cold TH-CREwt; *6–8*, TH-CREmu; *9–11*, TH-AP-1; *12*, buffer control for antibodies; and *13–15*, antibodies against CREB, ATF-2, and c-Jun, respectively. Data are representative from three to five independent experiments.

(Fig. 5*A*, *upper panels*), the level of the phosphorylated form of ATF-2 (on Thr^{71}) was increased without any significant change in the expression of ATF-2 (Fig. 5*A*, *lower panels*).

Previous mutation analysis of Thr^{69} and Thr^{71} of ATF-2 strongly indicated that the dual phosphorylated form of ATF-2, *i.e.* the protein phospho-Thr^{69} and -Thr^{71}, is the transcriptionally active form (35, 36). This form of ATF-2 was greatly increased in nuclear extracts of the V-1 clones, compared with that in those of the control clones (Fig. 5*B*). On the other hand, the amount of ATF-2 was not increased in the nuclear extracts of the V-1 clones (Fig. 5*B*).

We also used the GAL4 reporter assay to examine expression vectors expressing the transactivation domain of CREB or ATF-2 ($CREB_{TAD}$, amino acids 1–280 or ATF-2_{TAD}, amino acids 1–96, respectively) fused to a GAL4-DNA binding domain ($GAL4_{DBD}$). Although the $GAL4_{DBD}$-$CREB_{TAD}$ activity in the parental PC12D cells transiently co-transfected with a PKA expression vector was dramatically increased, this activity in the V-1 clones was unchanged compared with that in the control clone and the non-stimulated parental PC12D cells (Fig. 6*A*). In contrast, the $GAL4_{DBD}$-ATF-2_{TAD} activity in the V-1 clones was greatly increased and was comparable with that in PC12D cells transiently co-transfected with an active MEKK expression vector as a positive control (Fig. 6*B*). These data demonstrate that, ATF-2, as a TH-CRE-binding protein, was highly phosphorylated and activated in the V-1 clones.

Enhanced Activity of the TH Promoter in the V-1 Clones Was Attenuated by the Expression of the ATF-2 Transactivation Domain—To examine whether the enhanced activity of the TH gene transcription was due to activation of ATF-2, we adapted the $GAL4_{DBD}$-ATF-2_{TAD} expression vector to the reporter assay for the TH promoter. Overexpression of the $GAL4_{DBD}$-ATF-2_{TAD} protein containing the phosphorylation sites was expected to interfere competitively with the activation of the endogenous ATF-2 protein for the CRE-mediated TH gene transcription. The reporter activity of mTHpro0.8-Luc in the V1-69 clone was greatly decreased by co-transfection with the $GAL4_{DBD}$-ATF-2_{TAD} expression vector compared with that when the control vector that expressed $GAL4_{DBD}$ only was used for co-transfection, whereas that in the parental PC12D cells was slightly, but not significantly, decreased (Fig. 7*A*). The increased TH promoter activity in the V-1 clone remained unchanged by co-transfection with the $GAL4_{DBD}$-$CREB_{TAD}$ expression vector in

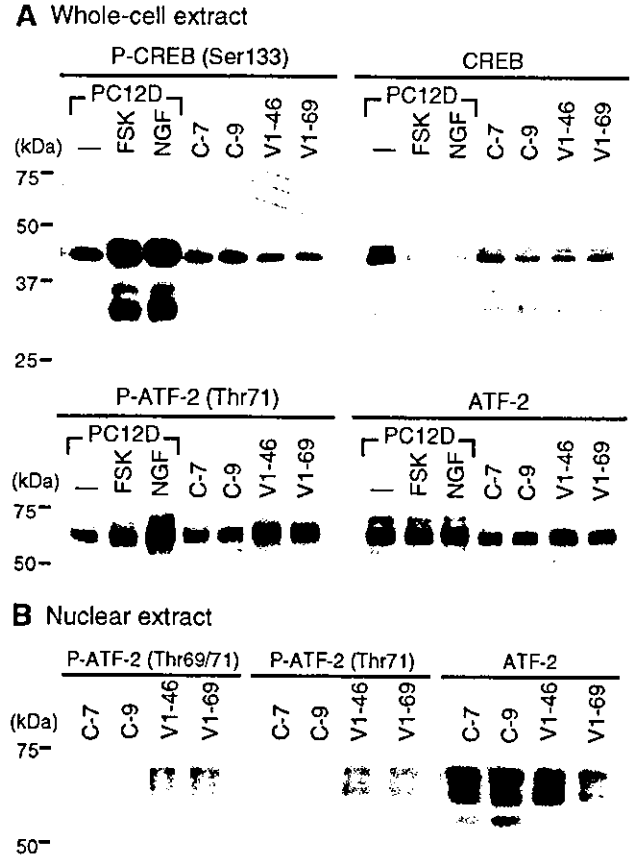

FIG. 5. **Phosphorylation of ATF-2 was increased in the V-1 clones.** Western blotting was performed using phosphorylated form-specific or nonspecific antibody against CREB or ATF-2. *A*, whole-cell extracts were prepared from PC12D cells incubated without or with 10 μM FSK or 10 ng/ml NGF and from V-1 or control clones. Whole-cell extracts were separated by SDS-PAGE (10% gel) and then analyzed by immunoblotting with antibodies against CREB phosphorylated on Ser^{133} and CREB (*left* and *right* of *upper panels*, respectively) or ATF-2 phosphorylated on Thr^{71} and ATF-2 (*left* and *right* of *lower panels*, respectively). *B*, nuclear extracts were prepared from V-1 and control clones and separated by SDS-PAGE (8% gel) and then analyzed by immunoblotting with antibodies against ATF-2 dual phosphorylated on $Thr^{69/71}$ (*left panel*), ATF-2 phosphorylated Thr^{71} (*middle panel*), and ATF-2 (*right panel*). Data are representative from three to five independent experiments.

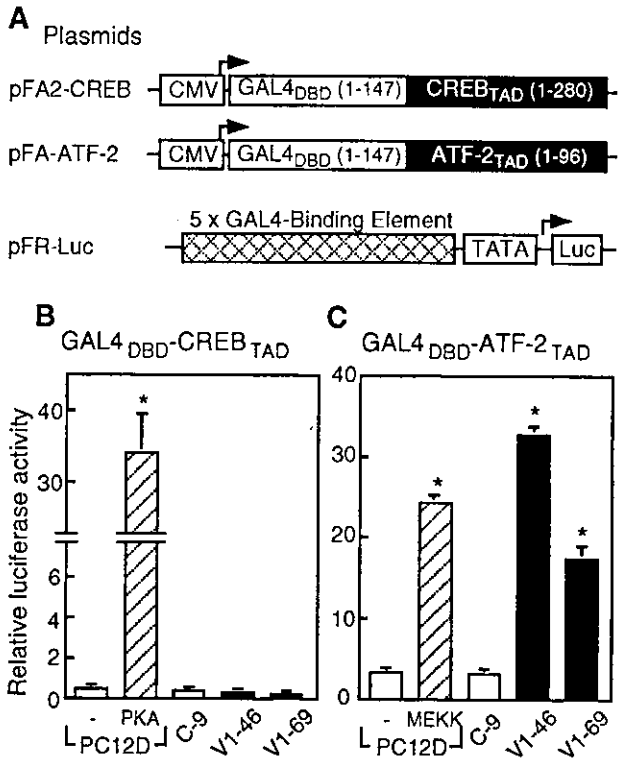

FIG. 6. **Activation of a GAL4-ATF-2 fusion protein in the V-1 clones.** *A*, expression vectors for fusion proteins (pFA2-CREB and pFA-ATF-2) consist of the transactivation domain of CREB and ATF-2 ($CREB_{TAD}$ and $ATF\text{-}2_{TAD}$, respectively) fused with the DNA binding domain of the yeast GAL4 ($GAL4_{DBD}$). The luciferase reporter vector (pFR-Luc) confers GAL4 responsiveness. *B*, the reporter activities in the presence of $GAL4_{DBD}$-$CREB_{TAD}$ (*A*) and $GAL4_{DBD}$-$ATF\text{-}2_{TAD}$ (*B*) were measured in the V-1 and control clones and in the parental PC12D cells. pRL-TK was used as an internal control to normalize for variations in transfection efficiency. As a positive control, PKA-expression vector (*PKA*) or a MEKK-expression vector (*MEKK*) was used for co-transfection of the parental PC12D cells. Data are the mean ± S.D. values from two independent experiments done in triplicate. Values of p were calculated based on the value of the parental PC12D cells: *, $p < 0.001$.

contrast to the $GAL4_{DBD}$-$ATF\text{-}2_{TAD}$ expression vector (Fig. 7*A*). In contrast to the TH promoter, the SV40 promoter was not activated in the V-1 clone and not affected by the expression of either $GAL4_{DBD}$-$ATF\text{-}2_{TAD}$ or $GAL4_{DBD}$-$CREB_{TAD}$ (Fig. 7*B*).

DISCUSSION

In the present study, we found that CRE-mediated transcription was highly elevated in V-1-overexpressing clones of the PC12D cell line. We then identified ATF-2 as one of the TH-CRE-binding proteins in PC12D cells, and, for the first time, found that activation of ATF-2 up-regulated the TH gene transcription via CRE.

ATF-2 (32), also called CRE-BP1 (34), is a member of the ATF/CREB family of transcription factors that bind to CRE. The TH-CRE was shown to be recognized by other members of the ATF/CREB family, *i.e.* CREB, ATF-1, and CREM (2–6). Among these transcription factors, only CREB was shown to be an activator of the TH gene transcription (7–10). Our data confirmed that CREB is one of the TH-CRE-binding proteins in PC12D cells (Fig. 4). However, our data showed that the enhanced transcription of the TH gene in the V-1 clones was driven by a CREB-independent mechanism, because neither CREB phosphorylation (Fig. 5) nor $GAL4_{DBD}$-$CREB_{TAD}$ activity (Fig. 6) was enhanced.

In contrast to CREB, we showed that ATF-2 was highly phosphorylated on Thr^{69} and Thr^{71} in the V-1 clones (Fig. 5) and that $GAL4_{DBD}$-$ATF\text{-}2_{TAD}$ activity was greatly enhanced (Fig. 6). There was no significant difference between the V-1 and control cells in expression level of ATF-2 determined by immunoblot analysis (Fig. 5) and in binding of ATF-2 to the TH-CRE determined by the gel mobility shift assay (data not shown). Because the $GAL4_{DBD}$-$ATF\text{-}2_{TAD}$ protein containing the phosphorylation sites had a dominant-negative effect for the enhanced activity of the TH promoter in the V-1 cells (Fig. 7), our data collectively show that phosphorylation of ATF-2 induced the TH gene transcription in the V-1 clones.

The stress-activated kinases (SAPKs), such as Jun amino-terminal kinase (JNK) (36) and p38/HOG (38), both of which phosphorylate ATF-2, have been identified as stimulators of ATF-2 (35, 36, 39). However the phosphorylation state or expression of these kinases in the V-1 clones was little changed compared with that of the control or parental PC12D cells, as determined by Western blotting analysis with antibodies against phosphorylated JNK or p38/HOG (data not shown). Although we have not yet identified the kinase that phosphorylates ATF-2 in the V-1 clones, a small up-regulation of these kinases may contribute to the long-lasting ATF-2 activation in the V-1 clones. Alternatively, there is a possibility that the

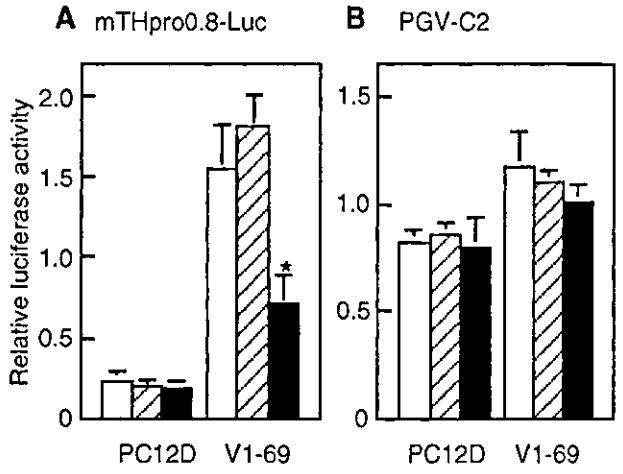

FIG. 7. **Enhanced activity of the TH promoter in the V-1 clones was attenuated by expression of ATF-2 transactivation domain.** Relative activities of the TH promoter vector (mTHpro4.3-Luc, *A*) and SV40 promoter vector (PGV-C2, *B*) were measured. The luciferase reporter vectors were used for co-transfection along with the expression vector for $GAL4_{DBD}$-$ATF\text{-}2_{TAD}$ (*closed bars*), $GAL4_{DBD}$-$CREB_{TAD}$ (*hatched bars*), or a control vector for $GAL4_{DBD}$ only (*open bars*); and pRL-CMV was used as an internal control to normalize for variations in transfection efficiency. The V1-69 clone and the parental PC12D cells were used. Data are the mean ± S.D. values from two independent experiments done in triplicate. Values of p were calculated based on the value of the control vector: *, $p < 0.001$.

activity of phosphatases active toward ATF-2, which have not been identified, may be decreased in the V-1 clones. It is of importance that the mechanism of the increased phosphorylation of ATF-2 in the V-1 clones be explored.

Our results suggest the involvement of phosphorylated ATF-2 in the enhanced CRE-mediated transcription in the V-1 clones. Although there are some reports showing enhancement of CRE-mediated transcription by phosphorylation of ATF-2 on Thr^{69} and Thr^{71} (40, 41), the mechanism is largely unknown. In the case of CREB, it is well known that phosphorylation of CREB on Ser^{133} directly recruits CBP, a transcriptional coactivator (42–44), and results in the transcriptional activation of the target gene. The transactivation domain of ATF-2, however, was reported not to interact with CBP even after phosphorylation (45). No protein has been identified as one that specifically binds to phosphorylated ATF-2 to elevate CRE-mediated transcription. The V-1 cells could be a good material to explore the mechanism.

ATF-2 was reported to bind not only to CRE, but also to AP-1 binding motif (33). Using nuclear extracts of striatal neurons, Guo *et al.* (46) found that ATF-2 bound to a TH-AP-1 oligonucleotide dissociated from the TH-AP-1 after the cells had been stimulated to induce TH expression. Since Band 1 containing ATF-2 was reduced in the presence of a TH-AP-1 competitor, though to a less extent than a TH-CRE competitor (Fig. 6, *lanes 9–11*), our data confirmed weak interaction of ATF-2 with the TH-AP-1. However, our data suggest that the TH-AP-1 does not contribute to the enhanced expression of the TH gene by the activated ATF-2 in the V-1 clones, because the activity of the AP-1-mediated transcription was unchanged in the V-1 clones (Fig. 2). NGF, a factor that induces differentiation of the sympathetic neurons in association with the expression of TH (47), preferentially activates the AP-1-mediated transcription in PC12 cells. It was reported that NGF-induced potentiation of the TH promoter activity was completely blocked by mutation of the TH-AP-1, but not by that of the TH-CRE (31), whereas enhanced activity of the TH promoter via the cAMP-PKA pathway was completely blocked by mutation of the TH-CRE (3, 31). The complete loss of the promoter activity in the TH-CRE mutant in the V-1 clones (Fig. 3) also suggests that AP-1-mediated transcription is independent of the enhancement of the TH gene transcription in the V-1 clones.

Mouse null mutants of ATF-2 died shortly after birth and displayed symptoms of severe respiratory distress with lungs filled with meconium (48). In the ATF-2-deficient mice, an increased level of TH mRNA was shown in the embryonic brain, and the authors attributed it to hypoxia in the mice (48). Our data, however, may suggest another possibility that it reflects a direct influence of the disappearance of ATF-2 for the TH gene expression.

Although ATF-2 was reported to be required for postnatal neural development (49), activation of ATF-2 was also observed in apoptotic cells, *i.e.* activation of ATF-2 reduced the survival rate of differentiated PC12 cells (50). There may be some unknown mechanisms of ATF-2 to regulate both apoptosis and differentiation of neural cells. Because the TH gene expression was induced by ATF-2 activation in the V-1 clones, these cells would be a good model for investigating the function of ATF-2 during neural development.

GTP cyclohydrolase I (GCH) is the rate-limiting enzyme for the *de novo* synthesis of tetrahydrobiopterin, which is an important regulator of TH enzymatic activity and the protein level (51). In the V-1 clonal cells, we recently showed an increased tetrahydrobiopterin content and enhanced expression of GCH (52). In our previous study, we showed increased promoter activity of the GCH gene in the V-1 clones (52) as we did for that of the TH gene in this report. Recently, ~150 bp of the 5′-promoter region of the GCH gene was identified as the region contributing to basal and cyclic AMP-induced transcriptional activity and containing a non-canonical CRE (28, 53), and we showed that this region was sufficient for the increased activity of the GCH promoter in the V-1 clones (52). Hirayama *et al.* (53) reported that the proximal promoter region could recruit ATF-2. These observations suggest that ATF-2 may coordinately regulate the expression of both TH and GCH genes.

It is interesting that the mRNA levels of AADC and DBH were also up-regulated in the V-1 clones (1), in addition to those of TH and GCH. Since the DBH gene has a noncanonical CRE in its 5′-flanking region to mediate cAMP-responsiveness (54); it is quite possible that the increased activity of the CRE-mediated transcription in the V-1 clones is responsible for the increased expression of the DBH gene. However, with the respect to the elevated expression of the AADC gene, the relationship between it and the CRE-mediated transcription has not yet been reported. Even though the expression of each enzyme might be governed by different transcription factors, any concerted regulatory mechanism(s) would be expected to play key roles during neural development. The present data suggest that ATF-2 may be involved in coordinate expression of the catecholamine-synthesizing enzymes for the development of catecholaminergic neurons.

In contrast to our observation of the enhanced expression of the catecholamine-synthesizing enzymes in the stable transformants of PC12D cells overexpressing V-1, transient transfection of PC12D cells with V-1 plasmids did not enhance the activities of the CRE- and TH promoter-reporting genes (data not shown). Because an increased expression of TH was observed in transgenic mice overexpressing V-1,[2] our data suggest that the enhanced expression of the TH gene may be a consequence of long lasting expression of V-1. Although we

[2] T. Yamakuni, T. Yamamoto, H. Yamamoto, S.-Y. Song, T. Nagatsu, K. Kobayashi, M. Yokoyama, A. Nakano, R. Suzuki, N. Suzuki, S. Iwashita, A. Omori, Y. Ichinose, C. Kato, M. Kobayashi, and Y. Ishida, unpublished observations.